Optimized Design and Structural Analysis of a Non-Pressurized Manned Submersible

by

Kenneth Shepard

B.S. Mechanical Engineering
Florida Institute of Technology, 1994

SUBMITTED TO THE DEPARTMENT OF MECHANICAL ENGINEERING IN PARTIAL FULFILLMENT OF THE REQUIREMENTS FOR THE DEGREE OF

MASTER OF SCIENCE IN NAVAL ARCHITECTURE AND MARINE ENGINEERING AND IN MECHANICAL ENGINEERING
AT THE
MASSACHUSETTS INSTITUTE OF TECHNOLOGY

JUNE 2011

Signature of Author:_____
Department of Mechanical Engineering
April 25, 2011

Certified by:_____
Mark S. Welsh
Professor of the Practice of Naval Construction and Engineering

Certified by:_____
John J. Leonard, Ph.D.
Professor of Mechanical Engineering and Ocean Engineering

Draper Advisor:_____
Peter Sebelius
Charles Stark Draper Laboratory

Accepted by:_____
David E. Hardt, Ph.D.
Professor of Mechanical Engineering
Chairman, Department Committee on Graduate Studies

(This page intentionally blank)

Optimized Design and Structural Analysis of a Non-Pressurized Manned Submersible

by

Kenneth S. Shepard

Submitted to the Department of Mechanical Engineering
on April 25, 2011in Partial Fulfillment of the
Requirements for the Degrees of Master of Science in
Naval Architecture and Marine Engineering and
Master of Science in Mechanical Engineering

Abstract

This thesis presents an approach to the structural design and optimization of a non-pressurized manned submersible (NPMS), a type of fully "flooded" submersible based on a SEAL Delivery Vehicle (SDV) Design Concept. Using the design parameters determined by the mathematical model, a solid model was generated and an ANSYS goal-driven optimizer was used to further optimize the hull weldment and variable ballast tanks. When three different designs were subsequently evaluated to verify the parametric model and the scalability of the NPMS design concept, all three were found to be able to be successfully generated and to meet the stated design requirements after ANSYS optimization. These findings indicate that the approach presented in this thesis can be used as an initial design tool in the future design of NPMSs.

Thesis Supervisor: Mark S. Welsh
Title: Professor of the Practice of Naval Construction and Engineering

Thesis Supervisor: John J. Leonard
Title: Professor of Mechanical Engineering and Ocean Engineering

(This page intentionally blank)

Acknowledgements

I would like to express my sincere gratitude to my MIT thesis advisors, Capt Mark Welsh and John Leonard, for their guidance and wealth of knowledge. This work was supported by the Charles Stark Draper Laboratory; and I'm truly grateful to have had the opportunity to with work with the SDV Optimization Study team with special appreciated to my sponsor, Pete Sebelius, for all the guidance he has imparted on me.

My education at MIT was made possible by my employer the United States Navy. I am truly gratefully to be associated with an organization which invests in the education of their people, and understands the importance of higher education.

Lastly, I am truly glad I had the opportunity to work with Paul Holzer. His operational experience and wealth of knowledge in this area was invaluable in completing this work.

(This page intentionally blank)

Table of Contents

List of Tables

List of Figures

Chapter 1 - Introduction, Background and Motivation

1.1 Introduction

This thesis examines an approach to the structural design and optimization of a non-pressurized manned submersible (NPMS), a type of fully "flooded" submersible that offers both simplicity and versatility in its application at a cost often significantly less than that of its pressurized counterpart. Due to these characteristics, the NPMS, including the SEAL Delivery Vehicle (SDV) MK 8 MOD 1 class developed by the U.S. Navy, has been established as a viable class of vehicle for the covert deployment of naval special operational forces (SOF) in a marine environment. The NPMS is typically designed to carry combatant swimmers and their required mission payloads submerged and undetectable to and from a prescribed target. As such, it is typically designed to cruise around 20 feet below the water surface but has the capacity to operate at multiple depths, as well as the capacity to be launched or recovered from various platforms, including surface ships, submarines, or pier sides, and to be transported by land, air, or sea. When submerged, the NPMS is fully flooded, leaving the passengers within exposed to ambient water temperatures and pressures and reliant on various underwater breathing apparatuses (UBAs). As the NPMS can be used to perform missions of a completely subsea nature, such as harbor penetration, it can act as a clandestine vehicle for locating combat swimmers within swimming range of a beachhead, harbor, or marine structure.

1.2 Background

The concept of employing a wet submersible to deploy submerged combatants for the purposes of executing highly specialized tasks can be traced back to the end of World War I. The Italian Royal Navy developed what it referred to as *human torpedoes*, essentially electrically propelled torpedoes used to deliver combat swimmers, colloquially known as *frogmen*, into enemy harbors. In 1918, the first known mission using this progenitor of submersibles was successfully completed when two combat swimmers rode a primitive human torpedo into the Austro-Hungarian Navy base of Pola and sank the Austrian battleship *Viribus Unitis* and the freighter *Wien* by planting mines [1].

During World War II, the Italian Royal Navy developed a class of wet submersible that they referred to as the *Maiale* as a means of transporting frogmen into a harbor or anchorage occupied by enemy ships. When close to the target, the frogmen would exit the NPMS, place a mine on the ship's hull, and return to the host submarine. One of the last remaining of this class of submersible, which the Italians used with great effectiveness against British ships anchored in Gibraltar [1], is on display at

the *USS Nautilus* Museum in Groton, CT and shown in Figure 1 [2]. The British developed their own class of submersible that they referred to as the *Chariot*, but used it with less success than did their Italian counterparts.

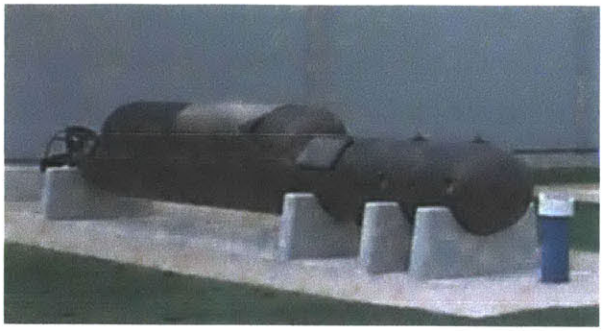

Figure 1: Italian "*Mailele*" Human Torpedo [2]

The U.S. Naval Special Forces entered the wet submersible field in the 1960s with their development of the Mark VII, a class of free-flooding submersible capable of transporting two frogmen and a small cargo relatively short distances [3]. Figure 2 shows an SDV Mark VII being lowered onto the *USS Grayback* [4].

Figure 2: The SDV MK 7Mod 6[4]

The Naval Special Forces followed their development of the SDV Mark 7 with the development of the SDV Mark 8 and Mark 9, shown in Figure 3, in the late 1980s. Whereas the SDV Mark 8 could transport six combat swimmers, the Mark 9 could transport only two combat swimmers but could also carry two MK 37 torpedoes. Currently, the SDV MK 8 MOD I is the only type of this class of submersible still in service, having been technically refreshed in the 1990s [5, 6]. A recent feasibility study conducted by Draper Laboratory and Massachusetts Institute of Technology aimed at identifying the means of optimizing NPMS capabilities through selective modifications within the

confines of the existing SDV vehicle envelope yielded a design concept that increased not only the cargo and payload capacity but also the diver capacity so as to accommodate eight combat swimmers, as illustrated in Figure 4 [7].

(a) (b)

Figure 3: SDV (a) MK 8[8] and (b) MK 9[2]

The US Navy has recently contracted for a replacement vessel for the SDV, the Shallow Water Combat Submersible (SWCS) [9], which is expected to remain in the design phase until it enters service in 2014.

Figure 4: Conceptual Illustration of optimized SDV MK 8 MOD 1[7]

1.3 Motivation

Despite the fact that decisions made in the earliest stages of the design of a vehicle tend to have the greatest impact on the outcome of the final design, the greatest emphasis is usually placed on the later detailed phases. In recognition of the importance of the early design phase, this study evaluates multiple early stage design concepts using the baseline NPMS design study [7] as a basis

for the development of a parametric mathematical model that can be utilized to explore the design space of similar vehicles. Use of this parametric mathematical model combined with a finite-element optimization method allows for the rapid identification of accurate solutions in a manner that is less computationally intensive than related methods.

Chapter Two - NPMS System Description

The baseline NPMS design examined in this thesis was developed from the design proposed by the NPMS design study [7], which had focused on increasing the number of combat swimmers that could be transported in an NPMS and its payload capacity without changing its overall dimensions. The NPMS basic design concept and subsystems are described in the remainder of the chapter.

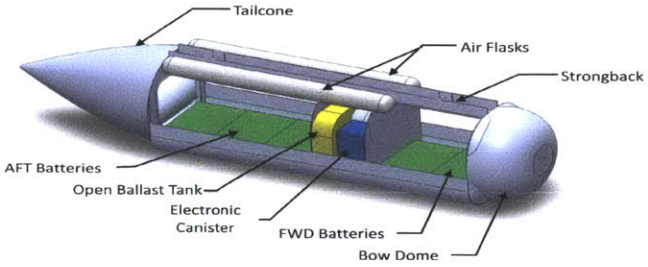

Figure 5: Basic NPMS configuration

2.1 Hull Subsystem

The NPMS hull subsystem consists of an aluminum mid-body hull weldment covered with composite and aluminum skins, an afterbody, and a bow. Defining the personnel and cargo compartments, the hull subsystem provides a structural surface for the attachment of the components and assemblies that constitute the other NPMS subsystems, contains built-in buoyancy pods that provide fixed buoyancy, and provides for the attachment of a lifting sling as a means of launching and recovering the NPMS with a hoist or crane. The hull subsystem is illustrated in Figure 6.

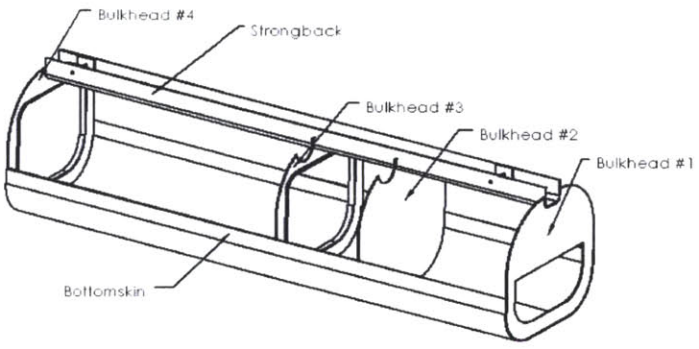

Figure 6: Hull subsystem configuration diagram

2.1.1 Strong back

As the primary structure of the NPMS, the strongback acts as its backbone. Constructed from 5086-H116 series aluminum, the strongback is a U-shaped beam running down the top of the NPMS that has two lifting sling attachments attached to each end, as well as four lifting-bearing plates (LBPs) centered on each of the lifting points welded to its inside to provide additional support during lifting (Figure 7). Bulkheads #1, #3, and #4 are welded to the strongback while bulkhead #2 is mechanically fastened. The strongback also houses a mast, sonar transducers, electronic sensors, pneumatic hoses, and control values.

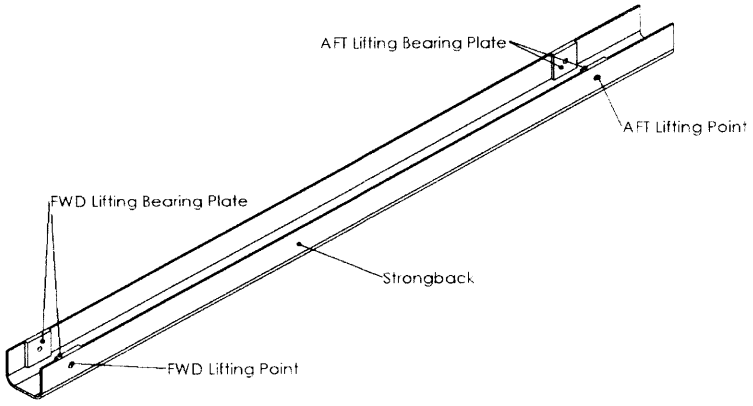

Figure 7: Structure of the Strongback

2.1.2 Bulkheads

The primary purpose of the bulkheads is to provide structural support and defines the profile of the NPMS. Bulkhead #1 provides the surface to attach the pilot displays and controls. Bulkhead #2 is constructed of either a composite or aluminum and is mechanically fastened to the strongback and the bottom skin. It provides a surface to attach various electronic canisters, control values and regulators. Bulkheads #3 and #4 are basically rings with a flange welded to the inside. The ring design allows the FBT to extend aft of bulkhead #3, if required, and allows diver access to the tailcone section for additional cargo stowage. Bulkhead #3 supports the forward end of the air flasks. Bulkhead #4 also supports the aft ballast tank, the aft end of the air flasks, and the tailcone.

2.1.3 Bottom skin

Constructed of 5086 H116 aluminum plate, the bottom skin provides the structure and fairing for the bottom of the NPMS and a surface to which to attach the four bulkheads and two longitudinal weldments.

2.1.4 Buoyancy Pods

Ideally, an NPMS can achieve neutral buoyancy, a state in which its weight is exactly equal to the buoyancy force acting on the NPMS, when its weight is exactly equal to the weight of water that it displaces. Unlike the hull of a submarine, which displaces a large volume of water and, consequently, yields a large buoyancy force, the hull of the NPMS displaces a small volume of water, resulting in its being in a state of negative buoyancy, which is undesirable [10].

To prevent the development of negative buoyancy, numerous buoyancy foam "pods" are distributed throughout the NPMS to allow it to achieve a neutrally buoyant condition while submerged. Comprised of a Divinycell® foam core, a buoyancy "pod" is coated with a protective layer of fiberglass and resilient paint and molded and shaped to form, and can be outfitted with fasteners or threads to aid in installation. The grade of Divinycell® form core depends on its pressure rating, and higher grades may be used for pods in vehicles designed to operate at deeper depths [11].

2.2 Mechanical Subsystems

Primarily operating on pneumatic power, the purpose of the NPMS mechanical subsystems is to allow for the performance of critical operations, primarily to operate the ballast and trim subsystem, to raise or lower the mast, provide auxiliary life support, and the operation of the drain values. Each subsystem is described in the sections that follow.

2.2.1 Ballast and Trim Subsystem

The Ballast and Trim (B&T) subsystem maintains the NPMS in the desired attitude and achieves neutral buoyancy during submerged operations under varying load conditions. The design concept presented in this study focused on increasing the capacity of the variable ballast tanks (VBT) and the available moment arm that can be used to compensate for various loads [7].

The B&T subsystem also provides a means for surfacing the NPMS by displacing water from the Open Ballast Tank (OBT) with High Pressure (HP) air or submerging the NPMS when surfaced by venting air from the OBT. The B&T system functional diagram is illustrated in Figure 8.

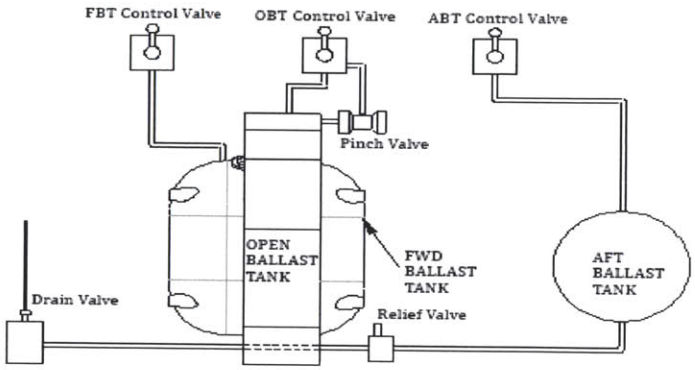

Figure 8: Ballast and trim system functional Diagram

2.2.1.1 Variable Ballast Tanks

The NPMS has two closed variable ballast tanks (VBTs), the forward ballast tank (FBT) and the aft ballast tank (ABT). Because the VBTs are located on both sides of the center of gravity of the NPMS, changing the relative water levels between them creates moment on the NPMS, which changes the trim. As such, water is shifted between the FBT and ABT to control the NPMS trim, and NPMS neutral buoyancy is achieved by flooding or venting the FBT and ABT. The locations of the VBTs in relation to the hull subsystem are shown in Figure 9.

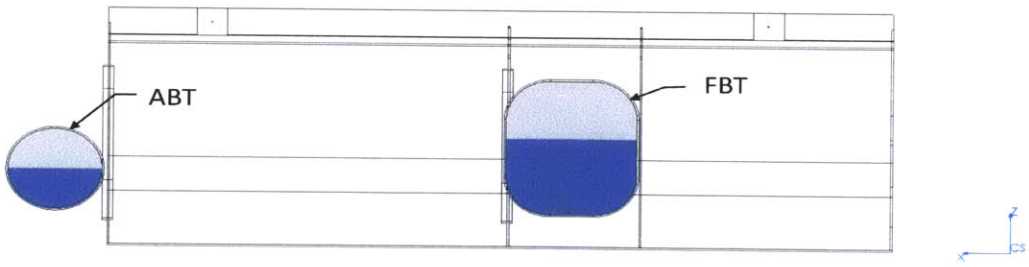

Figure 9: Variable ballast tank locations

Constructed of 5086 H116 aluminum alloy and supported from the longitudinal weldments, the FBT (Figure 10) is located between bulkheads #2 and #3 and electronic canisters are located on both sides that constrain the tanks width. Although the FBT can extend aft of bulkhead #3, its distance is minimized so that it does not constrain the aft crew compartment. The FBT contains two

upper boss sections that accommodate a liquid level indicator and an air-line fitting, and contains a drain pipe located on the bottom. The FBT is supported from the longitudinal weldments.

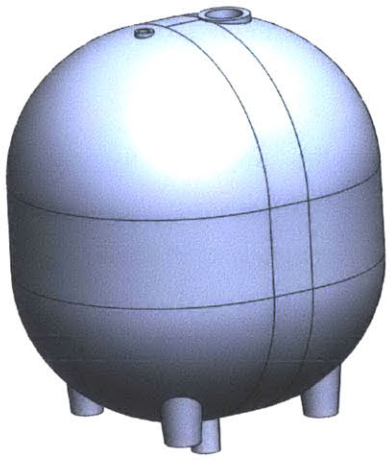

Figure 10: Forward Ballast Tank

Although also constructed of 5086 H116 aluminum alloy and containing the same two bosses and drain pipe, the ABT is typically smaller than the FBT (Figure 11). A cylindrical tank with elliptical ends, the ABT sits low in the NPMS, aft of bulkhead #4.

Figure 11: Aft Ballast Tank

2.2.1.2 Open Ballast Tank

The open ballast tank (OBT) is a non-pressurized tank open on the bottom that is flooded during submerged operations. When additional buoyancy is needed, operators force high pressure air into the OBT, forcing the water out and creating an on-demand buoyant "lift" force that serves primarily

as a safety feature. When the OBT is completely blown dry, several inches of the NPMS strongback remains out of the water, thus becoming a usable platform for diver recovery.

Located forward of bulkhead #3 and wrapping around the FBT, the OBT is fabricated from a composite material selected for its ease in manufacturing, light weight, and corrosion resistance.

2.2.2 Air Subsystem

The Air Subsystem provides auxiliary life support; pressurized air to the variable ballast tanks and pneumatic power to the mast. The NPMS Air Subsystem consists of two HP composite air flasks, a manifold, valves, fittings, hoses, and pressure transducer. The air flasks are located above the aft compartment and run parallel to the strongback.

2.2.3 Drain System

Designed to provide a means of draining the NPMS when it is being lifted from the water and flooding it when it is being lowered into the water, the drain system consists of two drain plates located on the bottom skin, centerline, between bulkheads #1 and #2 and between bulkheads #3 and #4.

2.3 Electronic and Propulsion Subsystems

The NPMS is powered by rechargeable battery cells housed in watertight battery boxes which are secured to the hull via the longitudinal weldment. The batteries supply power to a DC motor, controller assemblies and a single propeller. The NPMS Navigation Subsystem is comprised of a Commercial-off-the-Shelf (COTS) Doppler Velocity Log (DVL) and works by pulsing a sonar signal against the sea bottom or a water layer and measuring the Doppler shift of the returned signals [12]. The DVL sound head is located on the bottom of the vehicle. The Docking Sonar Subsystem provides a means for the NPMS to rendezvous with the host ship without visual contact. The system consists of docking sonar transponder which is located in the strongback and bow.

The NPMS Obstacle Avoidance Subsystem (OAS) provides the pilot and copilot a view of the water column in front of the vehicle. It consists of an OAS sound head located in the bow and attached to bulkhead #1 and the information is shown on displays attached to bulkhead #1. The NPMS communication systems provide internal and external communications. Antennas are located in a single pneumatically actuated mast that can be raised out of the water when surfaced. When not raised, the mast rests in the strongback. Several other electronic systems may be carried depending on the type of missions the NPMS is expected to perform.

Chapter 3 - Design Process

3.1 Design Process

Although the structural design of the NPMS is simple, the design space is quite large, ranging from a space designed for only a diver and co-pilot to a space for ten divers outfitted with various types of underwater breathing apparatus (UBA) who are carrying cargo of various sizes and weights and operating under multiple environmental conditions. It was quickly realized a parametric model (PM), which allows for determination of the direct relationships that define the hull structure and other components based on a set of design requirements, was the best means of fully investigating the NPMS design space. Moreover, it was recognized that use of the PM would also reduce some of the upfront computational costs while yielding a design sufficiently accurate to serve as an initial design.

An important aspect of designing the structures is the process of *optimization*, the application of a systemic method for determining the parameters that will yield the best possible design of a specific component while satisfying any physical or design constraint [13]. The parameterization of the structures is the key step in achieving a link between the structural analysis and the optimization. This study employed two optimization tools, MathCAD and ANSYS Finite Element Software. Selected on account of its ease of use, simplicity, capacity to provide solutions to constrained optimization problems, and integration with Excel and SolidWorks, MathCAD was used to develop the mathematical PM. The MathCAD PM provides the parametric relationships necessary to generate the hull profile, locate the bulkheads, size the VBTs and the air flasks, and conduct the initial optimization of the design. SolidWorks is a solid modeler that utilizes a parametric featured-based approach that can import the MathCAD design parameters into a pre-existing model. It provides the link between the MathCAD PM and ANSYS and generates the final solid model. Fully integrated with the parameterized solid model developed in SolidWorks, the ANSYS software contains a goal-driven optimization (GDO) module that uses the design parameters from the MathCAD model to optimize the geometries of the structure based on a set of goals and constraints [14].

The first step in the NPMS design process is identifying the design requirements for the NPMS, including the basic dimensional constraints, payload capacity, diver capacity, air flask volume, and environmental and operational constraints likely to be encountered. A particularly important design requirement is providing a level of structural safety that is based on a minimum acceptable

risk of failure. The model looks at two types of failure, stress and instability. To determine the acceptable margin between the yield strength of a material and the calculated stresses, a safety factor (SF) was used. To determine the acceptable margin from inelastic instability, the critical pressure (P_{crit}), the theoretical external pressure acting on a tank that leads it to buckle or become inelastically unstable, and the load multiplier *(LM)*, the value by which all the applied loads are multiplied to determine the theoretical load that causes buckling, were used. Although fatigue analysis is an important aspect of the design, it was beyond the scope of this thesis.

The next step in the design process is to generate the hull parameters in the MathCAD model. The model runs several constrained optimization routines to determine the preliminary sizing of the structural components by optimizing a cost function, such as calculated stress, while constraining parameters such as the strongback's height and width.

After the initial hull parameters have been determined, the FBT and ABT parameters can be generated. To do so, the MathCAD model again runs several constrained optimization routines to determine the preliminary geometries with the goal of minimizing the mass of the tanks while constraining the VBT volumes and stress.

The hull and VBT geometries from the MathCAD model are then imported into the SolidWorks PM to generate a 3D solid model. ANSYS imports the solid model, where external loads are applied to the structures, meshed and assigns material properties. The ANSYS design of experiments (DOE) module is used to generate a center composite design (CCD) based on selected key parameters and centered on the MathCAD design parameters. An FEA is performed on each of the design points and a response surface is generated.

The GDO module then uses the response surface and a set of goals and constraints to determine the means of achieving optimized design parameters, such as minimizing the weight and stress imposed on the ABT while keeping the tank volume constant. Using the results of the optimization, a final FEA is conducted with an increasingly finer mesh until a final solution is identified. Once the structure and VBTs have been optimized, the design parameters are imported back into the solid model, where the complete design is evaluated against the initial design requirements. The design process is summarized in Figure 12.

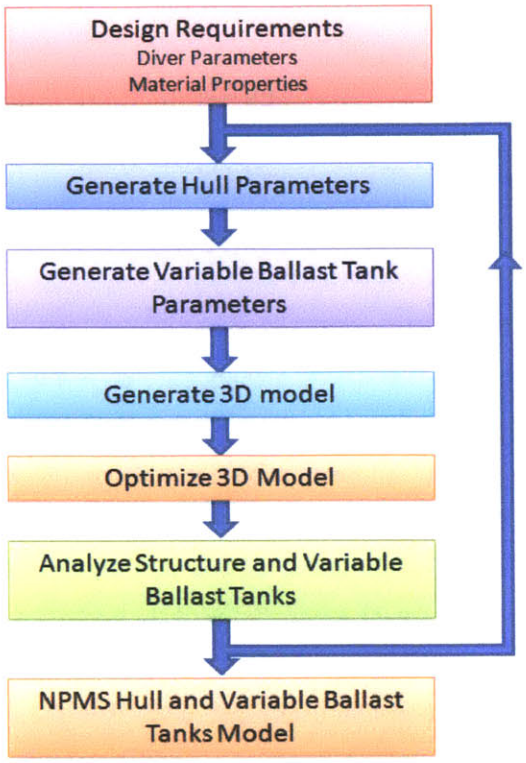

Figure 12: NPMS design process flow chart

Chapter 4 - Design and Analysis of Hull Subsystem

To provide the reader with understanding of the design and analysis methods used in this study, a notional non-dimensional design will be used in the following sections that describe how the variables flow through the design process and perform the calculations necessary to obtain the design parameters. The complete MathCAD PM is presented in Appendix A.

4.1 Design Inputs

The overall dimensions of the NPMS, which are defined by the maximum allowable length (L_{max}), the maximum allowable width (w_{max}), and the maximum allowable height (h_{max}), are typically constrained by its delivery method, which may depend on the size of the submarine dry dock shelter (DDS) or the transportation container, or on the deck space available on the support ship. In addition to the overall NPMS dimensions, the dimensions of the battery box, the length of the bow section (L_f), and the length on the parallel middle body (L_{PMB}) must be initially defined (see Figure 13). The L_f depends on the dimensions of the systems located in the bow (e.g., the OAS) and the legroom required for the diver and copilot, while the L_{PMB} depends on the number of divers, the volume of the electronic canisters, the battery dimensions, and the VBT requirements. L_{PMB} is initially estimated based on the design requirements and can be adjusted during the design process as required. The overall NPMS design parameters are non-dimensionalized by L_{max} and listed in Table 1.

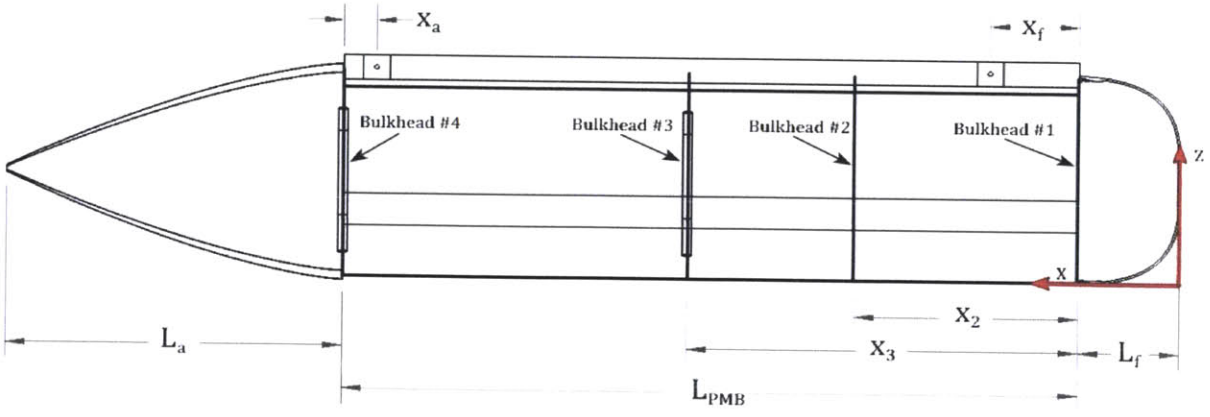

Figure 13: NPMS hull dimensions

Table 1: NPMS Design Parameters

Design Parameter	**Value/ L_{max}**
Maximum Vehicle Width (w_{max})	0.208
Maximum Vehicle Height (h_{max})	0.223
Maximum Length (L_{max})	1.000
Length of Parallel Midbody (L_{PMB})	0.635
Length of Bow Section (L_f)	0.090
Longitudinal Weldment Height (h_w)	0.012
Battery Dimensions (B_L x B_W x B_H)	0.138 x 0.09 x 0.035

Many of the design parameters depend on the physical properties of the combat divers transported within the NPMS. These include the minimum height (h_{Diver}) that a diver requires between the top of the battery and the underside of the air flasks, which depends on the average sitting height of the diver and the type of UBA he is expected to use; the minimum width (w_{Diver}) that a diver requires; the volume (V_{Diver}) that an individual diver occupies with his gear; the minimum stack length (L_{MDSL}), defined as the minimum longitudinal distance that a single diver requires in a compartment; and the diver stack length (L_{DSL}), defined as the minimum distance required between divers as measured from the front of one diver to the front of an adjacent diver.

An NPMS designed to carry a cargo of a certain weight and volume must meet requirements regarding the cargo wet weight (W_{cargo}), defined as the cargo's weight while submerged (weight less the buoyancy force), and the cargo volume (V_{cargo}), defined as the volume of water displaced by the cargo. The maximum operating depth (D_{max}) is defined by diver physiology and the maximum pressure the NPMS components are rated for. The diver and cargo design parameters are listed in Table 2.

Table 2: Diver and Cargo Design Parameters

Diver and Cargo Parameter
Minimum Diver Height (h_{diver})
Minimum Diver Width (w_{diver})
Minimum Diver Stack Length (L_{MDSL})
Diver Stack Length (L_{DSL})
Diver Volume (V_{diver})
Number of divers in forward compartment ($Divers_{fwd}$)
Number of divers in aft compartment ($Divers_{aft}$)
Air Flask Pressure (P_{AF})
Air Flask Volume (V_{AF})
Cargo Wet Weight (W_{cargo})
Cargo Volume (V_{cargo})

The expected change in the specific weight (sw) of water, which varies with the NPMS operational environment, is used to calculate the change in NPMS buoyancy and determine the size of the VBTs. The environmental design parameters are listed in Table 3.

Table 3: Environmental Design Requirements

Environmental Design Parameter	**Value**
Specific Weight of Water, Max (sw_{max})	64.5 lbf/ft^3
Specific Weight of Water, Nominal (sw)	64.0 lbf/ft^3
Specific Weight of Water, min (sw_{min})	62.5 lbf/ft^3

The hull and VBTs are constructed of 5086 H116 aluminum due to the strength and corrosion resistance arising from its temper, which is given a unique combination of cold work and thermal treatment to make it especially resistant to the corrosive effects of water and high humidity [15]. The buoyancy pods are constructed from Divinycell® H-grade foam based on a D_{max} [11] and the air flasks are constructed using wound carbon fiber filament. The material properties are summarized in Table 4.

Table 4: NPMS Material Properties

Material Property	**Value**
Poisson ratio (ν)	0.3
Yield strength, Al5086-O (YS_O)	17 ksi
Yield strength, Al5086-H116 (YS_{H116})	30 ksi
Elastic modulus, Al5086 (E_{5086})	10,300 ksi
Density, Al5086 (ρ_{5086})	0.096 lb/in^3
Yield Strength, Carbon Fiber (E_{CF})	819 ksi
Density, Carbon Fiber (ρ_{CF})	0.063 lb/in^3
Buoyancy Foam Density, (ρ_{foam})	7 lb/ft^3

4.2 Hull Weldment Worst Case Stress Scenario

The stress analysis on the hull weldment was analyzed under the worst case loading condition. In this scenario, the NPMS is filled with water to the top lip of the bottom skin and connected to a crane via the lifting sling, but still being support by the water. As the NPMS is being lifting out of the water, a large wave passes, causing the NPMS to be supported almost instantaneously from the lifting sling. The tension in the lifting sling experiences a force equal to exactly two times the weight of the NPMS, assuming that damping is negligible. Consistent with the American Petroleum Institute's standard, which states: "In the absence of a specified Significant Wave Height from the purchaser, offlead, sidelead, and wind forces shall be taken as zero, and the dynamic coefficient shall be taken as 2.0 [16]," a dynamic load factor (DLF) of 2.0 was applied to the structure analysis.

4.3 Bulkhead Placement

The internal bulkheads locations, X_2 and X_3, are determined by the diver stack length and based on the assumption that the divers are seated in rows of two. If the number of divers in the compartment is less than or equal to two, the minimum distance between the compartment bulkheads is equal to L_{MDSL}, whereas the distance between the compartment bulkheads depends on the L_{DSL} when more than two divers are in a compartment. The distances X_2 and X_3 are mathematically defined by Eq. (4.1) and Eq. (4.2), respectively.

$$X_2 = \begin{cases} L_{MDSL} & \text{if } Divers_{aft} \leq 2 \\ \left(\frac{Divers_{fwd}}{2}\right) L_{DSL} & \text{if } Divers_{aft} > 2 \end{cases} \quad (4.1)$$

$$X_3 = \begin{cases} L_{PMB} - L_{MDSL} & \text{if } Divers_{aft} \leq 2 \\ L_{PMB} - \left(\frac{Divers_{aft}}{2}\right) L_{DSL} & \text{if } Divers_{aft} > 2 \end{cases} \quad (4.2)$$

The forward and aft batteries are located between bulkheads #1 and #2 and between bulkheads #3 and #4, respectively, and are mechanically fastened to the longitudinal weldments. The bulkhead locations X_2 and X_3 are $.185L_{max}$ and $.331L_{max}$, respectively. Once the bulkhead locations have been determined, the required number of batteries to be placed in the forward and aft compartments is determined using the following formulas:

$$B_{fwd} = \text{trunc}\left[\frac{X_2}{W_{batt}}\right] \quad (4.3)$$

$$B_{aft} = \text{trunc}\left[\frac{L_{PMB} - X_3}{W_{batt}}\right] \quad (4.4)$$

where W_{batt} is the weight of a battery box.
Solving these equations reveals that two forward and three aft battery boxes are required.

4.4 Air Flasks

The air flasks are modeled as thin walled, circular cylinders with hemispherical ends. The hoop stress formula, Eq. (4.5), represents the maximum tangential stress in the air flasks, with the "meridional" or "axial" stress, Eq. (4.6), representing the stress in the longitudinal direction and in the hemispherical end caps [19].

$$\sigma_1 = \frac{Pr_{AF}}{t_{AF}} \quad (4.5)$$

$$\sigma_2 = \frac{Pr_{AF}}{2t_{AF}} \quad (4.6)$$

where:

P	Internal air pressure
r_{AF}	Air flask radius
t_{AF}	Air flask wall thickness

The air flask length (L_{AF}) must be greater than the distance between bulkheads #2 and #4 plus the radius of the air flasks (r_{AF}) to ensure that the air supply shut-off valve, located at the forward end

of the air flasks, is forward of bulkhead #2, and thereby accessible to the pilot and copilot. The minimum radius (r_{min}) and wall thickness (t_{AF}) are based on the manufacturer's capacity to produce a narrow cylinder of a given length. The value of the maximum radius (r_{max}) is selected to reduce the impact of the air flask in the aft compartment, based on the understanding that the larger the radius, the less vertical space is available to the rear divers. The constrained optimization problem is solved to minimize the air flask's mass according to the following constraints:

$$r_{min} \leq r_{AF} \leq r_{max}$$
$$t_{min} \leq t_{AF} \leq t_{max}$$
$$l \geq L_{PMB} - x_{BH2} + r_{AF}$$
$$\frac{YS_{CF}}{SF} > \sigma_1$$
$$\frac{4}{3}\pi {r_{AF}}^3 + \pi {r_{AF}}^2 l = V_{AF}$$

4.5 Bulkhead Profile

The requirement that the NPMS height (h_{NPMS}) must be equal to the minimum vertical stack height plus a height margin (h_{margin}) is mathematically expressed as:

$$h_{NPMS} = h_w + h_b + h_{MinDiver} + 2r_{AF} + h_{margin} \qquad (4.7)$$

This NPMS height must be confirmed to be less than h_{max}. Based on the assumption that the divers will be seated in rows of two, the bulkhead width (w_{BH}) is required to be equal to twice the minimum diver width plus a width margin (w_{margin}), and is calculated as follows:

$$w_{BH} = 2w_{diver} + w_{margin} \qquad (4.8)$$

The bulkhead profile is basically that of a rectangle with filleted corners (Figure 14), a configuration that allows for the formation of many profile shapes, from a rectangle to a circle, simply by varying the parameters.

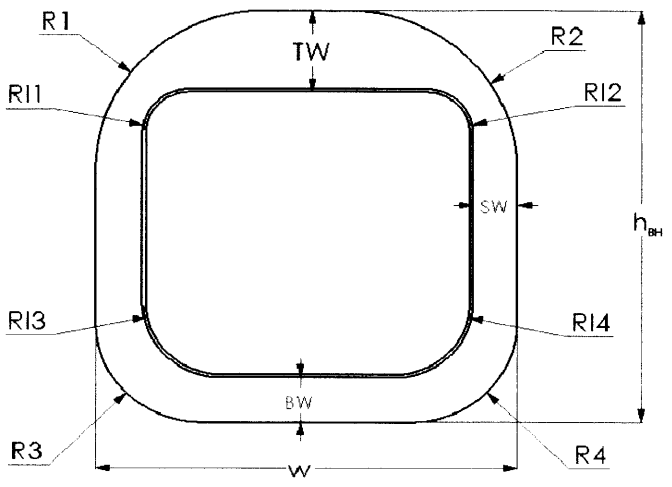

Figure 14: Bulkhead parameters

As functions of the battery length and the width of the NPMS, R3 and R4 are selected to ensure that the battery boxes can be fastened to the longitudinal weldments while maintaining sufficient space on the sides to ensure a drain path. The R1 and R2 dimensions depend on the width of the bulkhead and the air flask radius, based on the understanding that the air flasks will cut out the top portion of bulkheads #2 and #3. Setting TW equal to $2 \cdot r_{AF}$ ensures that sufficient material will remain to provide adequate structural support. The equations below can be modified as required conform to dry dock shelter cradle.

$$R3 = R4 = w_{BH} - B_L \tag{4.9}$$

$$R1 = R2 = \frac{w_{BH} - 2r_{AF}}{2}$$

$$RI1 = RI2 = \frac{w_{BH}}{9}$$

$$RI3 = RI4 = \frac{3}{4}R3$$

$$h_{BH} = h_{NPMS} - r_{AF}$$

$$TW = 2r_{AF}$$

$$SW = BW = RI1$$

4.6 Hull Profile

A basic hull profile is required to determine the overall volume envelope of the vessel, which is used to verify the hull has sufficient volume to house all the divers, cargo, buoyancy pods, and

subsystems. The hull profile is estimated by assuming the bow as a revolved segment of an ellipse, the tailcone as a revolved parabola, and center section as a parallel middle body. A true ellipse and parabola would make the lines too fine, so exponents are used to increase the fullness of the hull. The vertical offsets from its major axis are defined by [17]:

$$Z_{offset}(x) = \begin{cases} \left[1 - \left(\frac{L_f - x}{L_f}\right)^{\eta f}\right]^{\frac{1}{\eta f}} \frac{h_{BH}}{2} & 0 \le x \le L_f \\ \frac{h_{BH}}{2} & L_f \le x \le L_f + L_{PMB} \\ \left[1 - \left(\frac{x - (L_f + L_{PMB})}{L_a}\right)^{\eta a}\right] \frac{h_{BH}}{2} & L_f + L_{PMB} \le x \le L_{max} \end{cases} \quad (4.10)$$

The ellipse exponent coefficient (ηf) was set to 3.0 and the parabola exponent coefficient (ηa) was set to 1.75. The hull profile is plotted in Figure 15.

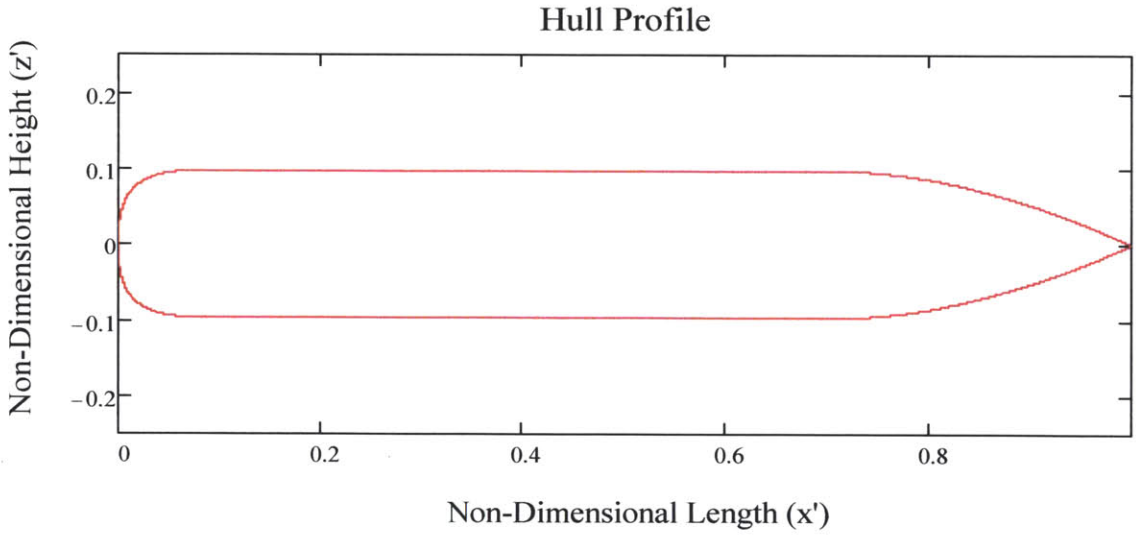

Figure 15: Hull Profile in the x-z plane

Once the hull profile has been determined, the volume of the hull envelope and the surface area are calculated using Eq. (4.11) and Eq. (4.12), respectively. Although these equations provide a close approximation of the volumes, the actual volumes will differ slightly because the actual bulkhead profiles are non-cylindrical.

$$V_{Hull} = \int_0^{L_f} Z_{Offset}(x)^2 \pi \, dx + A_m L_{PMB} + \int_{L_F+L_{PMB}}^{L_{max}} Z_{Offset}(x)^2 \pi \, dx \tag{4.11}$$

$$A_{Hull} = \int_0^{L} Z_{Offset}(x) 2\pi \, dx \tag{4.12}$$

where A_m is the cross sectional area of the parallel mid body.

The volume and CG_x of the bow and tailcone sections are determined using Eq. (4.13) through Eq. (4.16) and the mass of both sections are determined by multiplying the volume by their corresponding densities.

$$V_{bow} = \int_0^{L_f} \left(Z_{Offset}(x)^2 - \left(Z_{Offset}(x) - t_{tailcone} \right)^2 \right) dx \tag{4.13}$$

$$CG_{bow} = \frac{\int_0^{L_f} \left(Z_{Offset}(x)^2 - \left(Z_{Offset}(x) - t_{tailcone} \right)^2 \right) x \, dx}{V_{Tailcone}} \tag{4.14}$$

$$V_{Tailcone} = \int_{L_f+L_{PMB}}^{L} \left(Z_{Offset}(x)^2 - \left(Z_{Offset}(x) - t_{tailcone} \right)^2 \right) dx \tag{4.15}$$

$$CG_{tailcone} = \frac{\int_{L_f+L_{PMB}}^{L} \left(Z_{Offset}(x)^2 - \left(Z_{Offset}(x) - t_{tailcone} \right)^2 \right) x \, dx}{V_{Tailcone}} \tag{4.16}$$

4.7 Loads

Each bulkhead may have several system components attached to it. To simplify the analysis, the weights of a bulkhead's components are lumped into a single point mass (M_i) acting on each of the i^{th} bulkheads and illustrated in Figure 16. Bulkhead #2 is considered non-structural, and therefore loads are not applied to it. The center of gravity (CG) in the x-direction is calculated using Eq. (4.17) for each of the point masses.

$$CG_x = \frac{\sum (W \cdot CG)}{\sum W} \tag{4.17}$$

where:

W	Weight of a bulkhead component
CG	Center of Gravity (x) of a bulkhead component

For the assumption of at-sea recovery, the weight of the water contained within the hull (W_w) needs to be estimated. The water volume is assumed to be up to the top lip of the bottom skin minus the volume of the batteries. It is also assumed the weight of water in the bow or tailcone section is negligible and that the FBT does not displace any water.

As the W_w and the weight of the bottom skin (W_{BS}) are considered evenly distributed, the weight per inch (WPI) is defined as the total distributed weight acting on the bottomskin and determined using the following equation:

$$WPI = \frac{W_w + W_{BS}}{L_{PMB}}$$

The batteries are assumed to be two point masses, one for the forward battery boxes ($M_{fwdbatt}$) and one for the aft battery boxes ($M_{aftbatt}$) acting at $x_{fwdbatt}$ and $x_{aftbatt}$, respectively and illustrated in Figure 16.

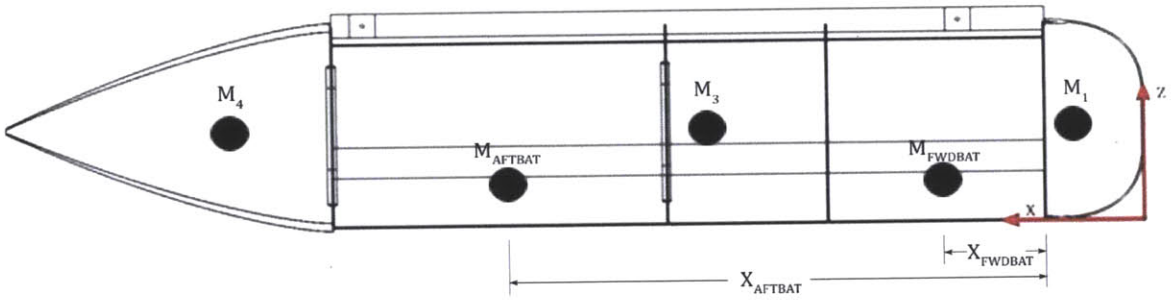

Figure 16: Point Masses

4.8 Strongback Design

The first step in determining the design of the strongback is to calculate the reaction forces on each set of lifting points. The following assumptions are made in determining the reaction forces:

- The bulkhead loads are assumed to be point loads as defined in section 4.7.
- The forward and aft vertical reaction forces are equal.
- The lifting sling forms a 45 degree angle with the strongback.

- The cargo and bulkhead weights are small compared to the weight of water and batteries and can be neglected.

The reaction forces, R_Z and R_x, are calculated using the expression:

$$R_Z = R_x = \frac{\sum M_i + WPI \cdot L_{PMB}}{2} \tag{4.18}$$

The next step in the strongback design process is to determine the optimized location of the lifting points, X_f *and* X_a, with the goal of minimizing the strongback's bending stress by minimizing the maximum moment placed on it, as illustrated in Figure 17. Simple beam theory is applied to calculate the moment on the strongback as a function of *x*.

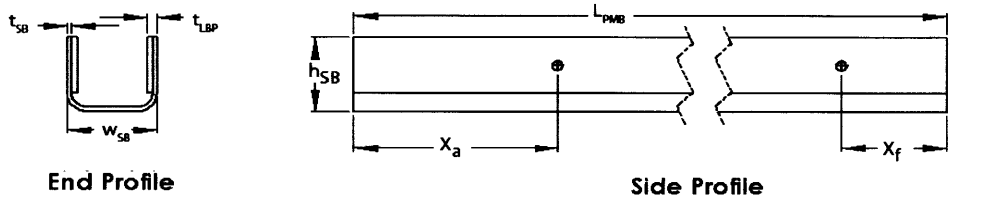

Figure 17: Strongback parameters

The strongback is modeled as "free-free" beam. The shear force, Q(x), in the beam is calculated according to $\int_0^x F(x)dx$, where F(x) is the force on an element of the beam [13]. Applying the integral to the loading yields:

$$Q(x) = \begin{cases} 0 & x < L_f \\ g \cdot M_1 + WPI\ (x - L_f) & L_f \le x < X_f \\ g \cdot M_1 + WPI\ (x - L_f) - R_y & X_f \le x < x_{fwdbatt} \\ g(M_1 + M_{fwdbatt}) + WPI\ (x - L_f) - R_y & x_{fwdbatt} \le x < X_3 \\ g(M_1 + M_{fwdbatt} + M_3) + WPI\ (x - L_f) - R_y & X_3 \le x < x_{aftbatt} \\ g(M_1 + M_{fwdbatt} + M_3 + M_{aftbatt}) + WPI\ (x - L_f) - R_y & x_{aftbatt} \le x < X_a \\ g(M_1 + M_{fwdbatt} + M_3 + M_{aftbatt} + M_4) + WPI\ (x - L_f) - R_y & x = L_f + L_{PMB} \end{cases} \tag{4.19}$$

where g is the acceleration of gravity.

The applied moment along the strongback, $M(x)$, is determined by $\int_0^x Q(x)dx$. A constrained optimization problem is set up to minimize the maximum moment on the beam by adjusting X_f *and* X_a given the following constraints:

$$\sum M_0 = 0$$

$$X_{fmin} < X_f < X_{fmax}$$
$$X_{amin} < X_a < X_{amax}$$

where M_0 is the moment about the point, x=0. The minimum and maximum constraints on X_f and X_a are determined by operator inputs and depends on arrangements in the strongback, such as mast and pneumatic control valves. Because the bulkhead point masses are not located directly under the bulkheads, couples are produced at both ends of the strongback. Point mass M_4 generates a significant couple because of its distance aft and weight. The shear and moment functions are plotted in Figure 17.

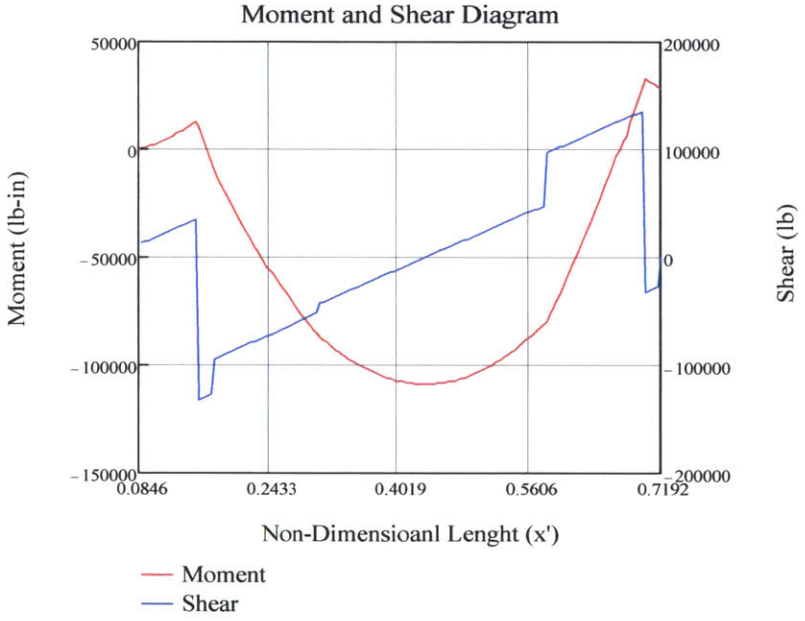

Figure 18: Strongback shear and bending moment diagram

The bending stresses on the strongback are small in comparison to the local stresses at the lifting points, as discussed in the following section. As the local stresses at the strongback lifting points tend to exert the strongest stresses on the strongback, they must be estimated in order to determine the optimal strongback dimensions.

Because of the complex stress interactions in this region, a response surface was constructed to predict the stress on the LBPs. The ANSYS DOE module was used to generate a center composite design (CCD) centered at the nominally expected design parameters. An FEA was performed on each of the design points and the maximum stress on the LBP was determined. A three degree polynomial response surface representing the LBP stress was fitted to the data which indicates that the stress is highly dependent on the strongback's height and the lifting hole diameter, and slightly dependent on the LBP thickness, as illustrated in Figure 19. The complete strongback results, including the ANOVA data, are presented in Appendix B.

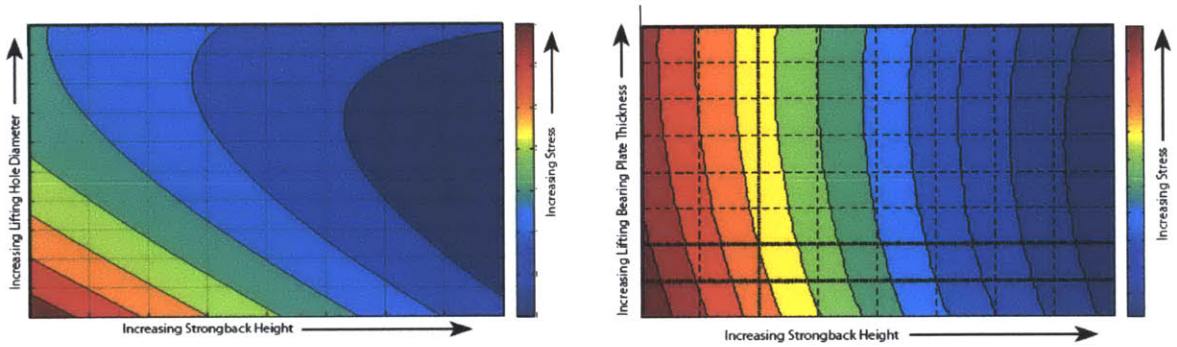

(a) (b)

Figure 19: Strongback lifting bearing plate stress by varying (a) strongback height and lifting hole diameter and (b) strongback height and lifting bearing plate thickness

The dimensions of the strongback ($\emptyset_{LP}, t_{LBP}, h_{SB}$) are determined by the stresses on the strongback and taking into account the shear stress on the lifting pin and using the following constraints:

$$\emptyset_{min} \leq \emptyset_{LP} \leq \emptyset_{max}$$

$$h_{min} \leq h_{SB} \leq h_{max}$$

$$t_{SB} \leq t_{LPB} \leq t_{max}$$

$$\frac{YS_{hull}}{SF} > \sigma(\emptyset_{LP}, t_{LBP}, h_{SB}), \quad \frac{YS_{pin}}{SF} > \frac{\sqrt{2}R_z}{\pi {\emptyset_{LP}}^2}$$

The minimum and maximum height of the strongback, h_{min} and h_{max} respectively, are selected based on the components housed in the strongback, i.e. the mast and sonar transducers. The

minimum lifting bearing plate thickness is set equal to the strongback's thickness. The maximum thickness (t_{max}) is limited again by the components housed in the strongback.

4.9 Bending Stress in Hull Weldment

The hull weldment bending stress is determined using the simple beam theory formula given by [13]:

$$\sigma_{Hull}(x) = \frac{M(x) \cdot z}{I_y} \tag{4.20}$$

where:

M(x)	Moment in hull
z	Distance from the neutral axis
I_y	Moment of inertia about neutral axis

The maximum bending stress of 137.8 psi, which occurs on the strongback at $.43L_{max}$., is well below the yield strength of the strongback. The bending stress in the hull weldment is plotted in Figure 20.

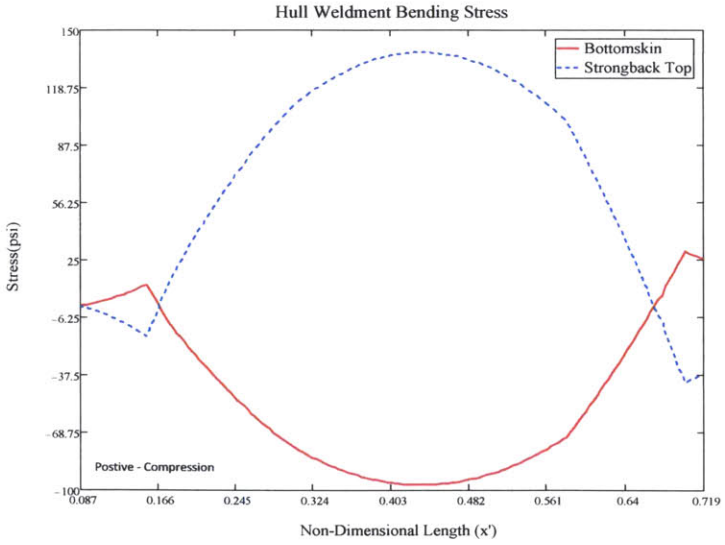

Figure 20: Hull weldment bending stress

Chapter 5 - Design and Analysis of the Closed Ballast Tank

5.1 Variable Ballast System design

The size of the VBTs depends on the weight of the cargo, the weight of the compressed air at maximum pressure, and the variation in buoyancy due to changes in water density. The required combined ballast tank water weight is given by:

$$V_{VBT} = \frac{1}{sw}\left[W_{cargo}\frac{sw_{max}}{sw_{min}} + W_{air} + W_{NPMS}\frac{sw_{max} - sw_{min}}{sw}\right](1 + VBT_{margin}) \quad (5.1)$$

where W_{NPMS} is the estimated weight of the NPMS and VBT_{margin} is the margin applied to the VBTs (VBT_{margin} =10%).

Based on the assumption that the cargo CG_x will be located at the vehicle CG_x, the VBTs are positioned and sized to create equal moments about the NPMS CG_x when both tanks are full. At this point in the process, the actual CG_x of the NPMS cannot be determined because the VBT masses are still unknown. The CG_x was parametrically estimated using the following equation:

$$CG_x = \frac{L_{max}}{3.70} + \frac{L_{PMB}}{4}$$

After the CG_x has been determined, the following equations are solved simultaneously:

$$V_{FBT}(CG_x - x_{FBT}) = V_{ABT}(x_{ABT} - CG_x) \quad (5.2)$$

$$V_{VBT} = V_{FBT} + V_{ABT}$$

The required OBT volume is based on a percentage of the VBTs. For this design, 25% was assumed to be sufficient to provide adequate buoyancy while surfaced. The VBT volume percentages are shown in Table 5.

Table 5: Variable Ballast Tank Volumes Percentages

Variable Ballast Tank	% VBT Volume
FBT	55 %
ABT	45 %

Unlike that of a typical submarine, the hull of an NPMS is not required to withstand external pressure. However, the VBTs, which are used to control the buoyancy and trim of the vessel, may be

subjected to an external pressure greater than the internal pressure. As a result, the external tanks are designed to withstand the hydrostatic pressure at the maximum operating depth with no internal pressure without elastic failure or buckling. Inelastic failure of the tanks would generate a shock wave, which could result in death or serious injury to the occupants [18].

The following assumptions are in VBT design analysis:

- The minimum collapse pressure (MCP) is 1.5 times the maximum operating pressure (MOP).
- The maximum peak stress, which includes the sum of all local stresses, is limited to the yield strength of the material divided by a safety factor (SF) of 2.0.

5.2 FBT Design and Analysis

The forward ballast tank (FBT) generally assumes the configuration of a rounded box with curved edges, a single vertical rib in the center, and a pair of front and side flat panels, as illustrated in Figure 21. By adjusting the parameters of the tank, the shape can be varied considerably to adjust to NPMS space constraints, which often require a compromise between the volume and allowable stress. For example, if the length and overall height of the tank is fixed, increasing F_O tends to decrease the stress on the tank while decreasing the internal volume. The goal is to find a solution to satisfy both volume and the stress limit.

Because the FBT shape is characterized by multiple curvatures and several flat sides, an accurate analytical solution is difficult to identify. To estimate the maximum stresses on the FBT membrane, which tend to occur on either the front or side panels, the ANSYS DOE module is utilized to construct a CCD for the range of expected design parameters.

The stresses on both panels were entered into MathCAD and two second degree polynomial response surfaces were fitted to the CCD results to predict the equivalent stress on the two panels. The FBT response surface results are presented in Appendix C.

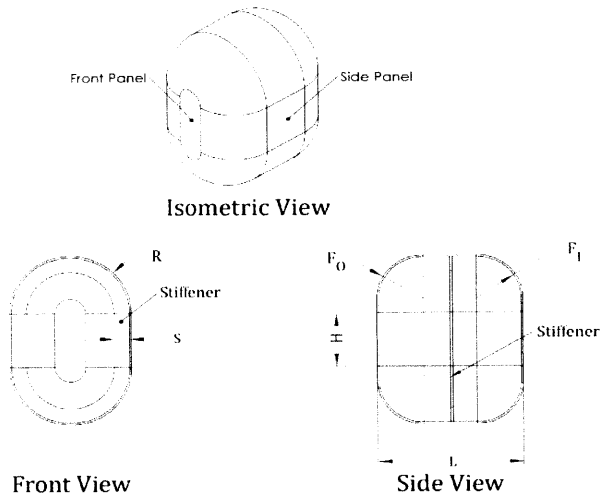

Figure 21: FBT dimensions

Once the stress functions have been determined, a constrained optimization routine is used to minimize the FBT mass. In the optimization process, the function, $\nabla(R, h, L, F)$, which is defined as the enclosed volume of the tank, is determined using the following equation:

$$\nabla(R,H,L,F) = (\pi R^2 + 2HR)L + \frac{4}{3}F^3 + 2\pi F^2(R-F) + 4F_O(R-F)(2R+H-2F) + \pi F^2(2R+H-2F) \quad (5.3)$$

Defined as the mass of the FBT taking into account the tank's center stiffener, the function $m(R, h, L, F_O, \mathrm{t}, \mathrm{S})$ is determined using the following equation:

$$m(R,H,L,F_O,\mathrm{t},\mathrm{S}) = \rho_{5086}\begin{bmatrix} V(R,H,L,F_O) - V(R-t,H,L-t,F_O-t) \\ + \left[2\pi\left(r-\frac{S}{2}\right)+2h\right]S\cdot t \end{bmatrix} \quad (5.4)$$

The optimization for the tank's mass is then determined by applying the following constraints:

$$R_{min} \leq R \leq \frac{w}{2}$$

$$\frac{R}{2} \leq F_0 \leq R$$

$$L_{FBT} < (X_3 - X_2) + x_d$$

$$H < \frac{L_{FBT}}{2.5}$$

$$H < h_{NPMS} - h_{SB} - h_{weldment} - 2R$$

$$t_{min} \leq t_{FBT} \leq t_{max}$$

$$\frac{YS}{SF} > \sigma_{side}(R, F_O, L_{FBT}, H, t_{FBT})$$

$$\frac{YS}{SF} > \sigma_{front}(R, F_O, L_{FBT}, H, t_{FBT})$$

$$V_{FBT} = V(R - t_{FBT}, H, L_{FBT} - t_{FBT}, F_O - t_{FBT}) - \left[2\pi\left(R - \frac{S}{2}\right) + 2H\right] S \cdot t_{FBT}$$

The limits on R and F_O are based on the range used for the response surface, as it may be highly inaccurate outside this range. The parameter L is limited to the distance between bulkheads #2 and #3 plus x_d, the acceptable distance that the FBT can extend aft of bulkhead #3. The first constraint is placed on H to prevent inelastic instability in the tank while the second constraint ensures that the tank will fit vertically in the space.

5.3 ABT Design and Analysis

The ABT is a special type of cylindrical pressure vessel in that its ends assume the form of an ellipsoid of revolution. The ABT parameters are shown in Figure 22. The stresses in the direction of the meridian and in the equatorial direction are given by Eq. (5.5) and Eq. (5.6) [19], respectively.

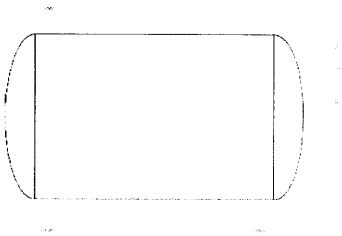

Figure 22: ABT parameters

$$\sigma_\theta = \frac{Pa}{t_{ABT}}\left(1 - \frac{a^2}{2b^2}\right) \tag{5.5}$$

$$\sigma_\varphi = \frac{Pa}{t_{ABT}} \tag{5.6}$$

where:

P	External pressure
t_{ABT}	ABT wall thickness

Because it is subjected to external pressure, the tank can fail due to elastic instability long before the compressive stresses reach a critical magnitude. The thinness ratio, which Blake [19] identifies as a key measure in determining the tank's response, is determined using:

$$\lambda = \frac{1.2m^{.25}}{(\kappa\phi)^{.5}} \tag{5.7}$$

where:

$$m = \frac{a}{t_{ABT}}$$

$$\phi = \frac{E_{5086}}{YS_{H116}}$$

$$\kappa = \frac{t_{ABT}}{L_{ABT}}$$

The response of the ABT when subjected to external pressure falls into two distinct patterns. The first response is characterized by circumferential lobes and localized buckling and the second by an hourglass shape. With λ values below 0.35, collapse due to instability is unlikely, whereas stability is the principal design consideration for values above 2.5. Therefore, the primary consideration for values between 0.35 and 2.5 is some combination of stress and instability [19].

There are considerable theoretical difficulties in analyzing a cylinder's vulnerability to external loads, especially in the thickness ratio range of 1.0 to 2.5, in which the ABT tends to fall [19]. For this reason the empirical formula Eq. (5.6) is used to calculate the critical buckling pressure on the ABT [19]. An advantage of using this formula is that the results cover a wide range of L/a ratios that do not require consideration of the length of the cylinder [19].

$$P_{crit} = YS_{5086} \cdot Z_1(Z_2 - nZ_3) \tag{5.8}$$

where:

$$Z_1 = e^{\left(\frac{-.815m^{.5}}{\kappa\phi}\right)}$$

$$Z_2 = {}^{1}/_{(m^{.95}(\kappa\phi)^{.10})}$$

$$Z_3 = \frac{50}{m^{1.95}(\kappa\phi)^{.10}} - \frac{33}{m^2}$$

To determine the optimal design of the ABT, the mass of the tank is defined according to:

$$m_{ABT} = \rho_{5086}\left[\left(\frac{4}{3}\pi a^2 b + \pi a^2 L_{ABT} - \left(\frac{4}{3}\pi(a - t_{ABT})^2(b - t_{ABT}) + \pi(a - t_{ABT})^2 L_{ABT}\right)\right)\right] \quad (5.9)$$

A constrained optimization is then established to minimize the ABT mass given the following constraints:

$$t_{min} \leq t_{ABT} \leq t_{max}$$

$$a \geq b$$

$$a < a_{max}$$

$$\frac{YS_{H116}}{SF} > \sigma_{\varphi}, \quad \frac{YS_{H116}}{SF} > -\sigma_{\theta}$$

$$V_{ABT} = \frac{4}{3}\pi((a - t_{ABT})^2(b - t_{ABT}) + \pi(a - t_{ABT})^2 L_{ABT}$$

$$MCP < P_{crit}$$

The limits placed on the tank's thickness (t_{ABT}) are based on the plate thicknesses available, their manufacturability, and the welding process. The minor radius (b) must be less than or equal to the major radius (a). The maximum value of a is selected to decrease the impact on the divers in the aft compartment, taking into consideration that if the tank extends excessively into their space, they will not be able to extend their legs over the tank to gain extra space in the aft compartment.

According to Timoshenko et al. [20] the extension of the radius of the cylindrical shell under the action of pressure (p) is given by Eq. (5.10) and the extension of the radius of the elliptical end is given by Eq. (5.11).

$$\delta_1 = \frac{pa^2}{Et}\left(1 - \frac{\upsilon}{2}\right) \tag{5.10}$$

$$\delta_2 = \frac{pa^2}{Et}\left(1 - \frac{a^2}{2b^2} - \frac{\upsilon}{2}\right) \tag{5.11}$$

From these two formulas it can be seen there is a discontinuity at the joints of the elliptical end and the cylinder. This indicates there is a shearing force and bending moment uniformly distributed along the circumference and of such magnitudes as to eliminate the discontinuity. The maximum axial (σ_x) and tangential stress(σ_t) in the cylinder are then given by [20]:

$$\sigma_x(\beta x) = \frac{ap}{2t} + \frac{3}{4}\frac{ap\frac{a^2}{b^2}}{t\sqrt{3(1-\upsilon^2)}}\zeta(\beta x) \tag{5.12}$$

$$\sigma_t(\beta x) = \frac{ap}{t}\left[1 - \frac{a^2}{4b^2}\theta(\beta x) + \frac{3a^2}{4b^2}\frac{\upsilon}{\sqrt{3(1-\upsilon^2)}}\zeta(\beta x)\right] \tag{5.13}$$

where:

$$\zeta(\beta x) = e^{-\beta x}\cos(\beta x)$$

$$\theta(\beta x) = e^{-\beta x}\sin(\beta x)$$

The values of σ_t and σ_x in the cylinder must be less than the allowable stress of the tank. When Eq.(5.12) and Eq.(5.13) were performed to determine the maximum stresses, $\sigma_x(\beta x)$ and $\sigma_t(\beta x)$, along the axial direction, $\sigma_x(\beta x)$ was found to be 2,664 psi and $\sigma_t(\beta x)$ to be 8,500 psi, both of which are well below the allowable stress of the tank.

Chapter 6 - Design Convergence and Optimization

6.1 Weight and Buoyancy Balance

Once the tank parameters have been calculated, the initial CG_x estimate is adjusted until it converges with the calculated CG_x value. After several iterations, the final CG_x was found to converge to $.457L_{max}$. The required buoyancy pod volume ($V_{Buoyancy}$) is then determined using:

$$\sum W_{comp} + Cargo_{wet} + \rho_{foam} \cdot g \cdot V_{Buoyancy} = SW \cdot V_{Buoyancy} + SW \cdot \sum V_{comp} \qquad (6.1)$$

where:

W_{comp}	Weight of a component
V_{comp}	Volume of a component

In order to minimize the trim on the NPMS, the center of buoyancy of the buoyancy pods (CB_x) is set equal to the CG_x. Finally, the total volume of all the components, cargo, and divers is compared to the volume bound by the hull profile to ensure that the NPMS is not volume limited.

6.2 Hull Weldment Finite Element Analysis

Once the MathCAD parametric model has converged on a solution, the hull weldment parameters are transferred into a SolidWorks parameterized solid model; where it can be imported into the ANSYS software.

The first step in modeling the hull weldment is to assign the correct weights to the vehicle. Point masses are added to the structure to represent the various masses not represented by the hull weldment. Point masses are attached to Bulkheads #1, #3 and #4 representing the total load on each bulkhead. The FBT mass was added to the Bulkhead #3 point mass previously calculated in section 4.7, and ABT mass was added to Bulkhead #4 point mass. In addition, two point masses were added to represent the forward and the aft batteries equal to their net weight in water. These point masses are illustrated in Figure 23.

The second step is to restrain the model by applying a cylindrical support to the forward and aft lifting points and applying constraints in the axial and radial directions. This type of support best approximates lifting the vehicle through the strongback's lifting points.

As the motions of the NPMS are accounted for quasi-statically, this was a general static analysis. The acceleration of gravity, which is multiplied by the DLF, is applied in the corresponding direction to allow the program to calculate the dynamic induced stress. This acceleration acts on the hull weldment and all the point masses described earlier.

A hydrostatic pressure is then applied to the bottom skin to simulate the weight of the entrapped water during a sudden lifting event. Because the general acceleration is not applied to the hydrostatic pressure, the fluid acceleration is set equal to acceleration of gravity multiplied by the DLF. The free surface of the water is set equal to the top lip of the bottom skin.

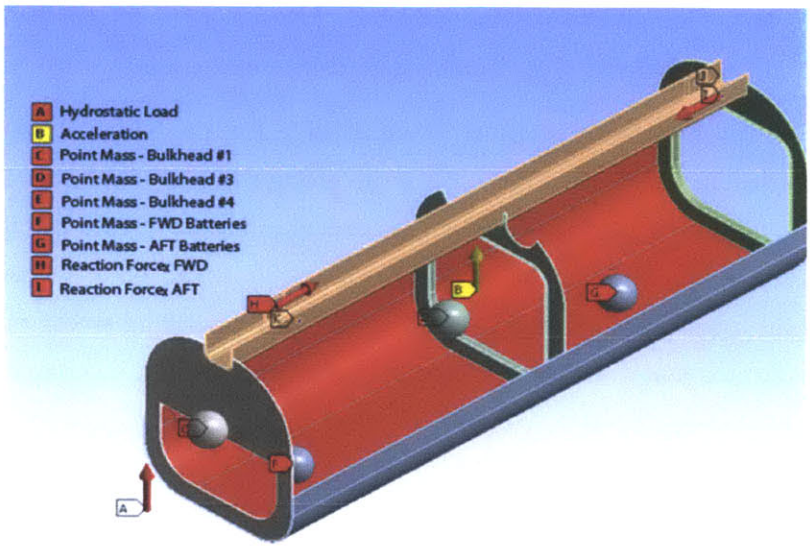

Figure 23: External loads on the hull weldment

An automatic mesh is applied to the hull weldment. Local mesh controls are applied to create a finer mesh near the vicinity of the lifting points and at the weld between the strongback and bulkhead #4, as these areas tend to have the largest stresses in the structure. The final mesh is illustrated in Figure 24.

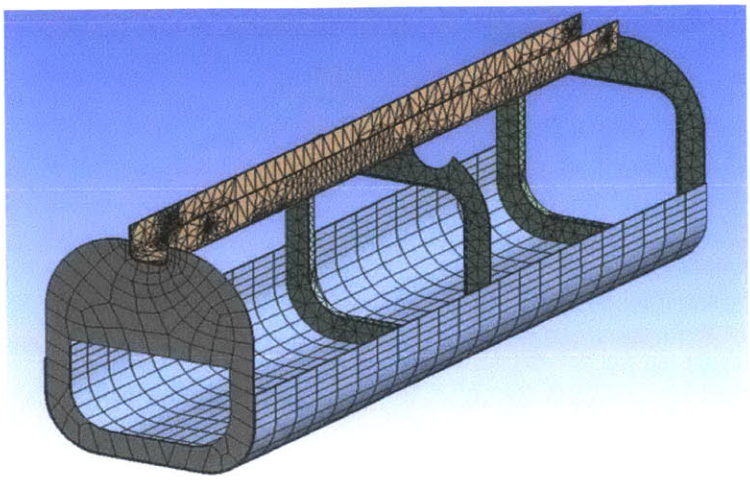

Figure 24: Hull weldment finite element mesh

Finally, a horizontal reaction force equal to the total weight of the NPMS is applied to each of the lifting points to represent the inward force from the lifting sling, as illustrated in Figure 25. When an initial FEA was performed, the maximum stress was found to be 19,260 psi at the weld between bulkhead #4 and the strongback, as illustrated in Figure 25. It can be observed that the moment created by the point mass attached to bulkhead #4 creates a bending stress on all the bulkheads and concentrates the stress at the weld between the bulkheads and the strongback.

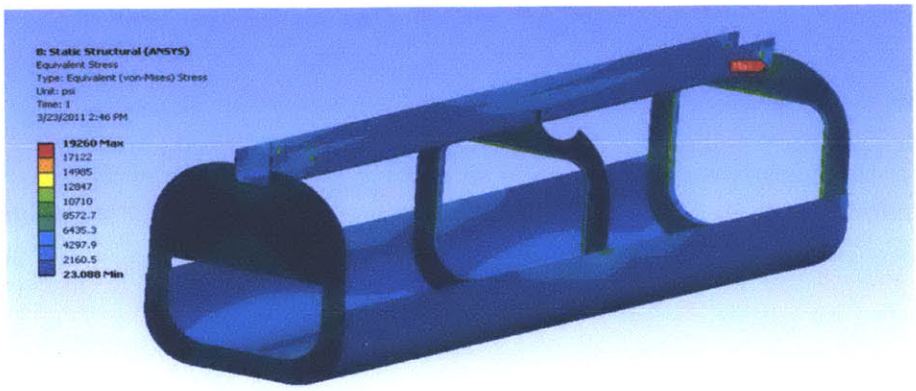

Figure 25: Hull weldment initial FEA results

6.2.1 Hull Weldment Optimization

The goal of the hull weldment optimization is to minimize the peak stresses and the mass of the hull weldment. As there are 14 design parameters that define the geometry of the hull, a full factorial design would encompass 16,413 design points. To simplify the problem and reduce the computational burden, the parameters of each of the three structural bulkheads can be set equal, i.e., the width of the sides can be assumed equal and symmetrical, and the bulkhead side width set equal to the bottom width. The optimization process can then be performed for the two subsets of the strongback and bulkhead parameter groups, whose parameters are relatively independent of each other. Following this procedure decreases the total design points to 58, vastly decreasing the computational time required.

The goal of the first optimization analysis is to minimize the peak stresses on the strongback using the ANSYS GDO module to identify the optimal LBP placement and dimensions. The parameters shown in Table 6 are varied in the DOE.

Table 6: Lifting Bearing Plate DOE Parameters

Strongback Parameter	Minimum Value	Maximum Value
X_a	0.500 X_a	1.500 X_a
X_f	0.500 X_f	1.500 X_f
$\emptyset_{LP}$	0.750 $\emptyset_{LP}$	2.000 $\emptyset_{LP}$
t_{LBP}	0.500 t_{LBP}	1.500 t_{LBP}
SB_H	0.750 SB_H	1.250 SB_H

When the second optimization was performed, the maximum stress on the LPB decreased from 17,781 psi to 14,555 psi, and although the maximum stress remained located at the weld between the strongback and bulkhead #4, it decreased from 19,260 psi to 18,552 psi, as illustrated in Figure 26.

Figure 26: Strongback optimization results

The goals of the second optimization analysis are to reduce the overall weight of the weldment, minimize the maximum stress, and minimize the height of the bottom skin. Decreasing the bottom skin height reduces the weight of the water in the hull but can also produces higher bending stresses in the bulkheads.

Table 7: Hull Weldment DOE Parameters

Bulkhead parameter	**Minimum Value**	**Maximum Value**
BS_H	0.50 BS_H	1.00 BS_H
TW	0.75 TW	1.00 TW
SW	0.75 SW	1.00 SW

After the second optimization, the stress in the weld between the strongback and bulkhead #4 decreased to 14,707 psi, as shown in Figure 27.

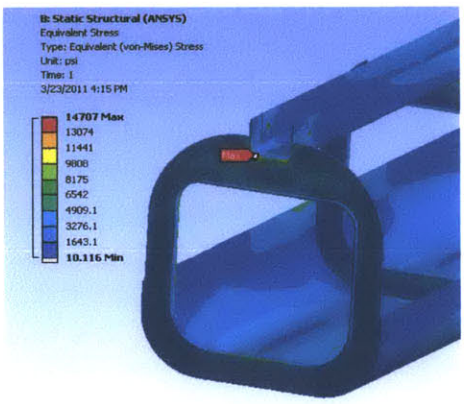

Figure 27: Bulkhead optimization results

6.2.2 Hull Weldment Results

Because the maximum stress occurs in the weld-affected zone, the yield strength in the weld-affected zone is reduced to that of 5086-O aluminum and the allowable stress to 11,333 psi when a SF of 1.5 is applied. To decrease the stress in this region, a plate is welded to the end of the strongback. After performing an additional FEA with the new end plate, the maximum stress on the weld is located on the forward LBP and decreased to 14,001 psi, well below the allowable stress limit. The results of both optimization analyses are summarized in Table 8.

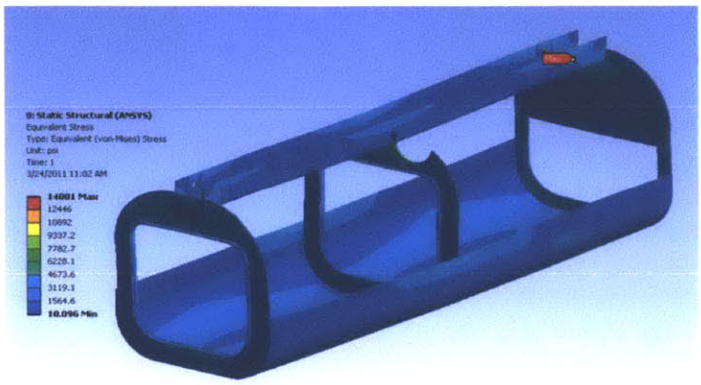

Figure 28: Final finite element analysis on the hull weldment

Table 8: Hull Weldment Results

	Parametric Model	**Initial FEA**	**Optimizer Prediction**	**Final FEA**
	X_f		0.764 X_f	
	X_a		1.500 X_a	
	$\emptyset_{LP}$		1.136 $\emptyset_{LP}$	
	t_{LBP}		0.556 t_{LBP}	
	SB_h		1.078 SB_h	
	TW		0.846 TW	
	SW		0.755 SW	
	BS_H		0.75 BS_H	
Mass/PM Mass	1.000	0.889	0.873	0.857
Maximum Stress	18,976 psi	19,260 psi	16,421 psi	14,001 psi

6.3 FBT Finite Element Analysis

Once the MathCAD parametric model has converged on a solution for the tank parameters, the parameters are imported into the SolidWorks model. ANSYS is then used to apply an external

pressure load to the external faces equal to the MCP. The tank is fully restrained on one of the side panels. A mesh is applied to the tank with a relevance of 10, which results in 7,764 nodes and 17,284 elements, as illustrated in Figure 29. The tank is assigned material 5086 H116 Aluminum.

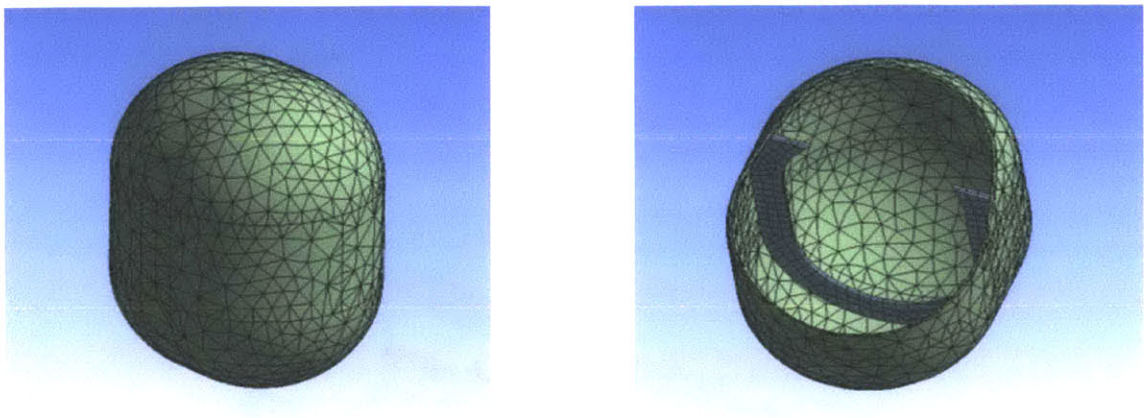

(a) (b)

Figure 29: FBT finite element mesh (a) external view and (b) internal view

6.3.1 FBT Design Optimization

Using the ANSYS DOE module, a DOE is constructed according to a CCD that varies the design parameters listed in Table 9.

Table 9: FBT DOE Parameters

FBT Parameter	Minimum Value	Maximum Value
R	1.000 R	1.000 R
F_O	0.833 F_O	1.000 F_O
F_I	0.750 F_I	1.000 F_I
L_{FBT}	0.950 L_{FBT}	1.050 L_{FBT}
t_{FBT}	0.667 t_{FBT}	1.250 t_{FBT}
S	0.750 S	1.250 S

The optimization module is then used to converge on a final design in which the mass and maximum stresses are minimized while the tank's internal volume is kept constant. The optimized design parameters are then entered into the model to perform a complete FEA to confirm the results. The results are summarized in Table 10 and illustrated in Figure 30.

Table 10: FBT Results

	Parametric Model	Initial FEA	Optimizer Prediction	Final FEA
	R		1.000 R	
	F_O		1.000 F_O	
	F_I		1.010 F_I	
	t_{FBT}		0.668 t_{FBT}	
	L_{FBT}		0.998 L_{FBT}	
	H		1.086 H	
	S		0.833 S	
Mass/m_{FBT}	1.000	1.013	0.746	0.709
Volume/V_{FBT}	1.000	0.998	1.068	1.047
Maximum Stress	6,026 psi	5,052 psi	8,325 psi	7,938 psi
Buckling LM	N/A	58.9	20.2	22.8

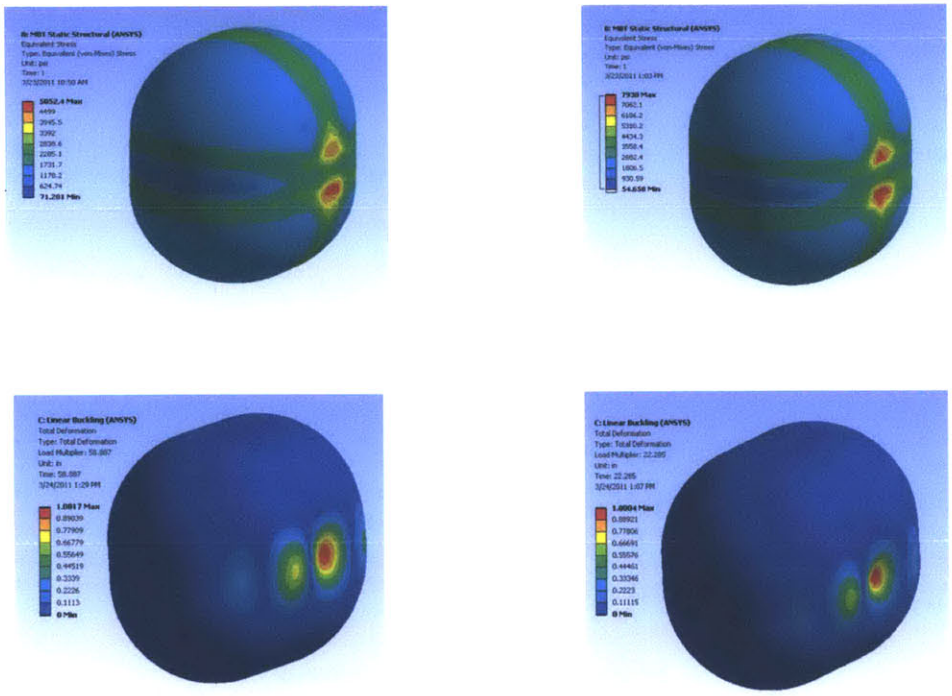

(a) (b)

Figure 30: FBT finite element results for (a) initial and (b) post-optimization analysis

6.4 ABT Finite Element Analysis

After the MathCAD model has converged on a solution, the ABT parameters are transferred into the SolidWorks model. ANSYS software is then used to mesh the ABT and an external pressure load is applied to the external faces equal to the MCP. The edge between the cylinder and the elliptical end is assumed in the x, y and z directions, and the opposite edge is fixed in the y and z-axis. A mesh is applied to the tank with a relevance of 5, which results in 11,712 nodes and 5,877 elements (Figure 31). The material property assigned is that of 5086 H116 Aluminum which has been presented section 4.1 in this paper.

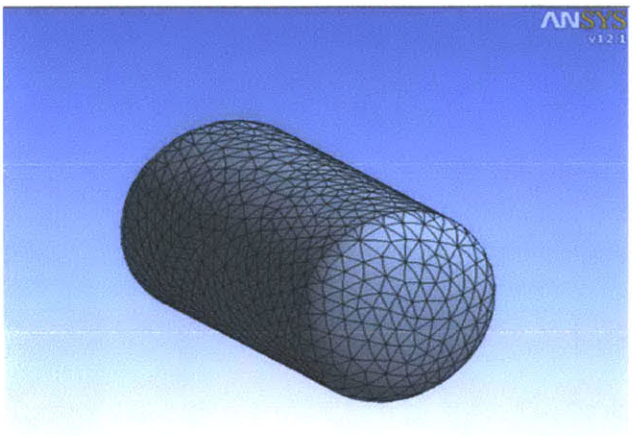

Figure 31: ABT finite element mesh

6.4.1 ABT Design Optimization

The same optimization process is used for the ABT except there are only 4 DOE parameters. The DOE parameters are listed in Table 11.

Table 11: ABT DOE Parameters

Design Parameter	Minimum Value	Maximum Value
a	0.90 a	1.10 a
b	0.75 b	1.25 b
t_{ABT}	0.67 t_{ABT}	1.00 t_{ABT}
L_{ABT}	0.75 L_{ABT}	1.25 L_{ABT}

Using the ANSYS GDO module, the tank is optimized by setting the goals to minimize the mass and stress while maintaining the ABT volume constant. A final FEA is then performed that includes a linear buckling analysis of the optimized design parameters. The non-dimensional results are summarized in Table 12 and graphically shown in Figure 32.

Table 12: ABT Results

	Parametric Model	**Initial FEA**	**Optimizer Prediction**	**Final FEA**
	a		1.035 a	
	b		1.183 b	
	t_{ABT}		1.000 t_{ABT}	
	L_{ABT}		0.867 L_{ABT}	
Mass/m_{ABT}	1.000	1.043	1.105	1.054
Volume/ V_{ABT}	1.000	1.013	0.982	0.993
Maximum Stress	10,099 psi	8,054 psi	5,568 psi	5,991 psi
LM	2.6	12.5	13.0	13.0

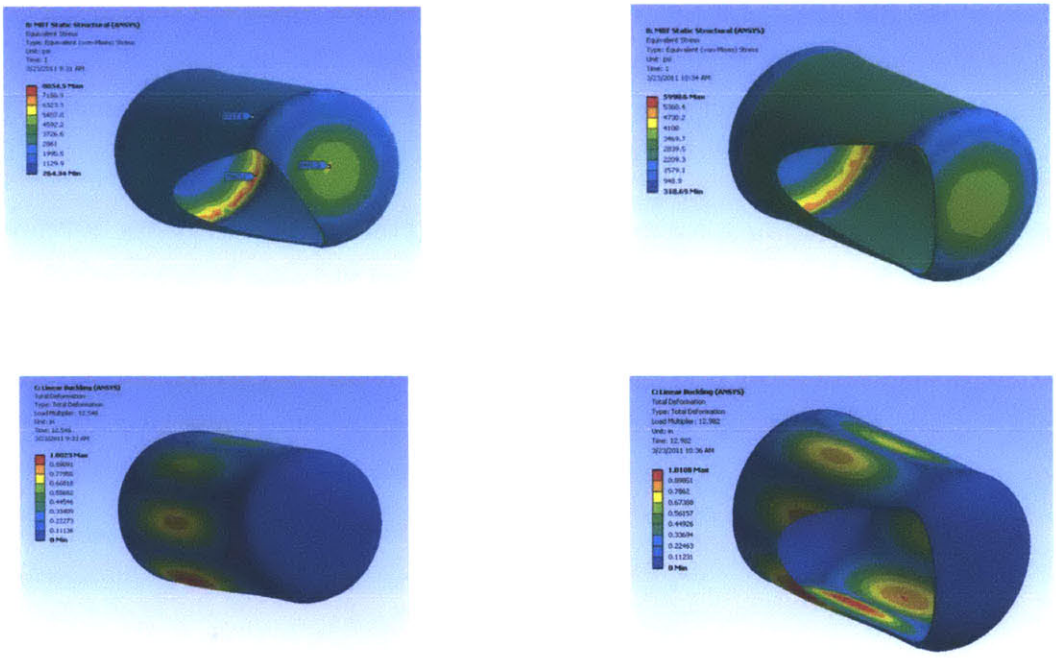

(a) (B)

Figure 32: ABT finite element results for (a) initial and (b) post-optimization analysis

6.5 Final NPMS Design Results

Comparison the hull weldment results reveals that the initial solid model mass was 11.1% less than that of the PM. The initial FEA maximum stress on the LBP was 1,195 psi less than that predicted by the PM. After the ANSYS optimization had been performed, the mass of the hull weldment decreased by 3.6% and the maximum stress decreased by 4,553 psi. After reinforcing the aft end of the strongback, the maximum stress in the hull weldment decreased to 14,001 psi.

In general, the stresses in the hull weldment are considerably less than the yield strength, as predicted by the simple beam theory in section 4.9, with higher stress regions occurring at the union between the bulkheads and the strongback, which were not modeled by the PM.

Comparison of the PM FBT results with the initial FEA results reveal that the solid model mass was 1.3% heavier, the volume .2% less, and the maximum stress 974 psi less than those of the PM. After performing the FEA optimization, the solid model mass decreased by 30%, the volume increased by 5.9%, the maximum stress increased by 2,886 psi, and the buckling LM decreased by 36.1.

Comparison of the PM ABT results with the initial FEA results reveal the solid model mass was 4.3% heavier, the volume 1.3% larger, and the maximum stress 2045 psi less than the PM. After the FEA optimization, the solid model mass increased by 1.1%, the volume decreased by 2.0%, the maximum stress increased by 2,063 psi, and the buckling LM decreased by .5.

The ANSYS optimization resulted in a total weight savings that equates to a 21% increase in cargo weight capacity. After optimization of the hull weldment and VBTs has been performed, the NPMS is assembled using the optimized parameters. The battery boxes, electronic canisters and the OBT are added to the model to verify that the components can be properly placed within the structure. The midsection between bulkheads #2 and #3 contains ample room to house electronic boxes, OBT, DVL, buoyancy pods and cabling. A cross-sectional view of the final design is presented in Figure 33.

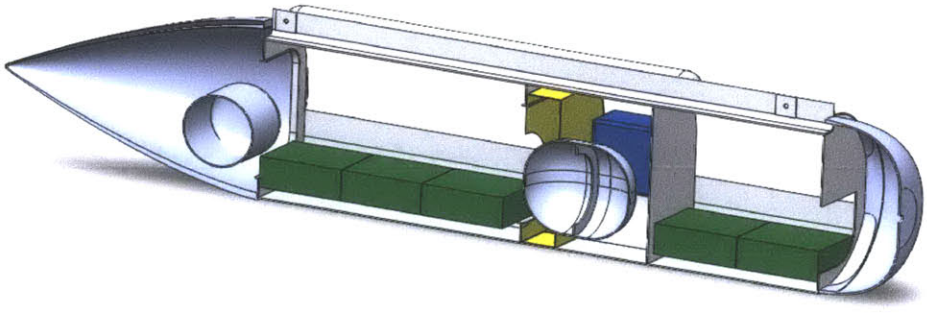

Figure 33: Final NPMS design concept sectional view

Chapter 7 - Design and Model Verification

7.1 Design models

In this chapter, two additional designs are evaluated to ensure the scalability of the PM. Design #1 is the model developed in the previous chapters; design #2 is a smaller design that can accommodate six combat divers with limited gear or cargo; and design #3, the longest of the three designs, accommodates up to ten divers, has a large cargo capacity, and operates at the deepest operating depth. Despite their differences, all three designs

- utilize the same electronic and sonar systems,
- operate in the same ocean environments, and
- use the same materials.

Designs #2 and #3 were designed and analyzed using the same method described in previous chapters. The design requirements for each design are summarized in Table 13.

Table 13: NPMS Design Requirements

Design Requirement	Design #1	Design #2	Design #3
Maximum Width	w_{max}	0.963 w_{max}	1.037 w_{max}
Maximum Height	h_{max}	0.966 h_{max}	1.034 h_{max}
Maximum Length	L_{max}	0.865 L_{max}	1.154 L_{max}
Length of Parallel Midbody	L_{PMB}	0.813 L_{PMB}	1.152 L_{PMB}
Cargo Wet Weight	W_{cargo}	0.833 W_{cargo}	1.667 W_{cargo}
Cargo Volume	V_{cargo}	0.600 V_{cargo}	1.600 V_{cargo}
Min Diver Height	h_{diver}	1.000 h_{diver}	1.031 h_{diver}
Max Operating Depth	D_{max}	0.667 D_{max}	1.333 D_{max}

7.2 Design #2 Results

Design #2 has the shortest length of the three designs, being able to accommodate only four batteries. Moreover, the mid-body section between bulkheads #2 and #3 is more compressed than that of the other designs, leaving less space for buoyancy pods and electronics. As the aft cargo space is reduced, only four divers can occupy the aft compartment, and only the pilot and copilot can occupy the forward compartment.

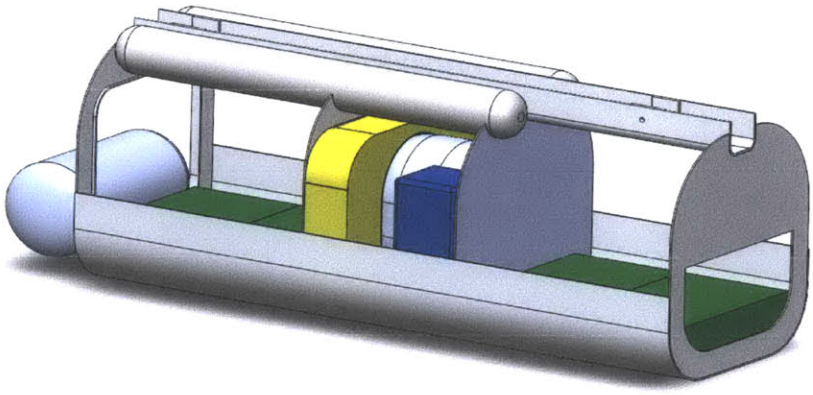

Figure 34: Design #2 solid model

Due to its shorter length, design #2 bears less stress at the weld of the strongback and bulkhead #4, with the strongest stress occurring on the forward LBP. After performing strongback optimization, the maximum stress is located at the weld of bulkhead #1 and the strongback and is reduced to 14,208 psi, which exceeds the allowed yield strength of the weld area. To further decrease the stress, an aluminum plate is welded to the bulkhead to reduce the stress on the weld to less than 8,000 psi, as shown in Figure 35. After the final optimization, the highest stress (10,545 psi) is located on bulkhead #4. The results are summarized in Table 14.

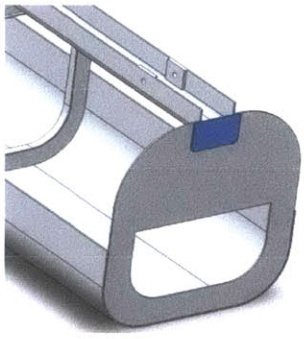

Figure 35: Forward strongback end plate

Table 14: Design #2 Hull Weldment Results

	Parametric Model	**Initial FEA**	**Optimizer Prediction**	**Final FEA**
	X_f		1.001 X_f	
	X_a		0.921 X_a	
	$\emptyset_{LP}$		1.600 $\emptyset_{LP}$	
	t_{LBP}		1.250 t_{LBP}	
	SB_h		1.143 SB_h	
	TW		0.067 TW	
	SW		0.849 SW	
	BS_H		0.900 BS_H	
Mass/PM Mass	1.000	1.002	0.882	0.873
Maximum Stress	14,981 psi	12,793 psi	11,455 psi	10,545 psi

The required VBT volume is 15% less than that required by design #1 and the FBT and ABT volume percentage is 55% and 45%, respectively. The FBT and ABT FEA results are summarized in Table 15 and Table 16, respectively.

Table 15: Design #2 FBT Results

	Parametric Model	**Initial FEA**	**Optimizer Prediction**	**Final FEA**
	R		1.000 R	
	F_O		1.046 F_O	
	F_I		1.048 F_I	
	t_{FBT}		1.000 t_{FBT}	
	L_{FBT}		1.040 L_{FBT}	
	H		1.023 H	
	S		1.000 S	
Mass/m_{FBT}	1.000	1.004	1.025	1.013
Volume/V_{FBT}	9,907 in^3	.961	1.019	1.012
Maximum Stress	5,326 psi	5,439 psi	5,236 psi	5,346 psi
Buckling LM	N/A	68	55	64

Table 16: Design #2 ABT Results

	Parametric Model	Initial FEA	Optimizer Prediction	Final FEA
	a		1.012 a	
	b		1.077 b	
	t_{ABT}		1.000 t_{ABT}	
	L_{ABT}		0.953 L_{ABT}	
Mass/m_{ABT}	1.000	1.013	1.109	1.060
Volume/ V_{ABT}	1.000	1.000	1.002	0.996
Maximum Stress	3,105 psi	2,813 psi	2,637 psi	2,557 psi
Buckling LM	2.7	19.5	18.53	19.53

7.3 Design #3 Results

The third design extends the length of the NPMS to 300 in. This considerably increases the aft cargo capacity and 8 divers are expected to fit in the compartment. The additional length allows for 4 battery boxes in the aft and two in the fwd compartment.

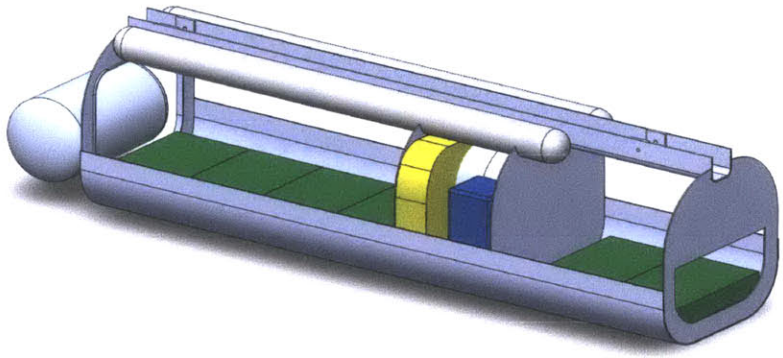

Figure 36: Design #3 solid model

During the initial FEA, the maximum stress on the structure occurred at the aft LBP. After the optimization was performed, the stress on the LBP was reduced to 12,755 psi. As the maximum stress occurred at the weld between the strongback and bulkhead #4, a plate was welded to the aft end of the strongback to reduce the stress in this region. The final maximum stress now occurs on bulkhead #3, as illustrated in Figure 37. The results are summarized in Table 17.

Table 17: Design #3 Hull Weldment Results

	Parametric	**Initial FEA**	**Optimizer**	**Final FEA**
	X_f		1.233 X_f	
	X_a		1.313 X_a	
	$\emptyset_{LP}$		1.667 $\emptyset_{LP}$	
	t_{LBP}		1.278 t_{LBP}	
	SB_h		1.036 SB_h	
	TW		0.851 TW	
	SW		0.776 SW	
	BS_H		0.750 BS_H	
Mass/PM Mass	1.000	0.928	0.917	0.901
Maximum Stress	19,930 psi	27,012 psi	19,128 psi	18,831 psi

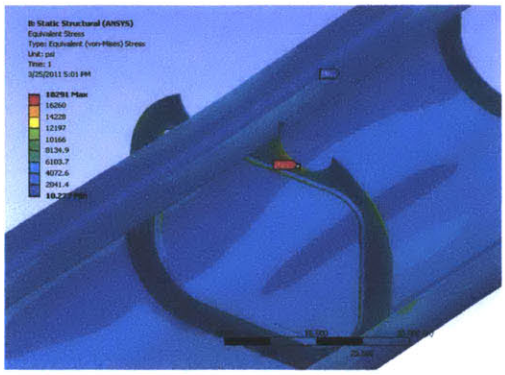

Figure 37: Design #3 final FEA showing location of maximum stress

Due to the cargo capacity and size of the NPMS, the total variable ballast required is 65% larger than design #1, 52% of the volume in FBT and 48% of the volume in the ABT. The stress in the FBT is the largest of the three FBT and is close to the allowable stress limit for this tank design. FBTs larger then this would require a second internal stiffener to decrease the stress on the side plates. The results of the VBTs are summarized in Table 18 and Table 19, respectively.

Table 18: Design #3 FBT Results

	Parametric	Initial FEA	Optimizer	Final FEA
	R		1.000 R	
	F_O		0.914 F_O	
	F_I		0.900 F_I	
	t_{FBT}		1.333 t_{FBT}	
	L_{FBT}		0.988 L_{FBT}	
	H		1.010 H	
	S		1.100 S	
Mass/m_{FBT}	1.000	0.996	1.321	1.343
Volume/V_{FBT}	1.000	.975	1.044	.993
Maximum Stress	15,000 psi	18,550 psi	11,215 psi	14,141 psi
LM	N/A	8.8	19.4	8.5

Table 19: Design #3 ABT Results

	Parametric	Initial FEA	Optimizer	Final FEA
	a		0.976 a	
	b		1.100 b	
	t_{ABT}		1.000 t_{ABT}	
	L_{ABT}		0.974 L_{ABT}	
Mass/m_{ABT}	1.000	1.063	1.079	1.048
Volume/ V_{ABT}	1.000	1.052	1.007	1.024
Maximum Stress	11,389 psi	9,912 psi	7,039 psi	7,565 psi
LM	1.3	397	772	564

Chapter 8 - Conclusion and Future Work

8.1 Conclusion

This thesis presented an approach to optimizing the design and structural analysis of an NPMS using an SDV design concept parameterized into a mathematical and 3D solid model that allowed for several constrained optimizations of the hull weldment and VBTs. Using the design parameters determined by the mathematical model, a solid model was generated and an ANSYS goal-driven optimizer was used to further optimize the hull weldment and VBTs. When three different designs were subsequently evaluated to verify the PM and the scalability of the NPMS design concept, all three were found to be able to be successfully generated and to meet the stated design requirements after ANSYS optimization. These findings indicate that the method presented in this thesis can be used as an initial design approach for the development of NPMSs in the future.

On average, performing optimization according to the FEA results decreased the mass of the hull weldment by 6% and the stress by 31% from the initial solid model. In two instances, an additional plate had to be attached to the end of the strongback to reduce the stress on the weld. The differences between the models at each stage in the hull-weldment design process are summarized in Table 20.

Table 20: Differences between Design Models in Hull Weldment Design

	Maximum Stress		Mass	
	Difference between PM and initial FEA	Difference between Initial and Final FEA	Difference between PM and initial solid model	Difference between initial and final solid model
HW #1	1%	-38%	-11%	-3%
HW #2	-15%	-15%	0%	-13%
HW #3	36%	-41%	-7%	-3%
Average	7%	-31%	-6%	-6%

The stress levels for the FBT in designs #1 and #2 were found to be well below the allowable stress limits. Although FBT stress level of the PM of design #3 approached the FBT stress limit and the stress level in the initial FEA was above the limit, the FBT stress level was within the allowable stress after FEA optimization. Indeed, all three FBT designs were able to meet the design requirements after FEA optimization. However, as the FBT stress limit was approached even after optimization, larger tanks will require the addition of another stiffener. As the design for the

smallest tank, design #2 allowed for more optimization compared to other two designs. A comparison of the design differences between the models during the FBT design process is summarized in Table 21.

Table 21: Summary of FBT design differences

	Maximum Stress		Volume		Mass	
	Difference between PM and initial FEA	Difference between initial and final FEA	Difference between PM and initial solid model	Difference between initial and final solid model	Difference between PM and initial solid model	Difference between initial and final solid model
FBT #1	-13.3%	49.5%	-0.2%	4.9%	2.4%	-30.7%
FBT #2	2.1%	-1.7%	-3.9%	5.1%	0.4%	0.9%
FBT #3	23.7%	-29.4%	-1.0%	-0.9%	8.2%	6.9%
Average	4.2%	6.1%	-1.7%	3.1%	3.7%	-7.7%

The PM was found to over predict the stress placed on the ABT by an average of 15%, but very closely estimate the ABT mass and volume. The optimization results were found not to yield any significant benefits compared to the original solid model. A comparison of the design differences during the design process is summarized in Table 22.

Table 22: Differences between Design Models in ABT Design

	Maximum Stress		Volume		Mass	
	Difference between PM and initial FEA	Difference between initial and final FEA	Difference between PM and initial solid model	Difference between initial and final solid model	Difference between PM and initial solid model	Difference between initial and final solid model
ABT #1	-20.2%	-34.2%	1.3%	-2.0%	5.2%	-4.1%
ABT #2	-9.4%	-8.2%	0.0%	-0.5%	4.6%	1.3%
ABT #3	-15.5%	16.7%	-0.5%	-2.2%	-3.2%	9.7%
Average	-15.1%	-8.6%	0.3%	-1.6%	2.2%	2.3%

8.2 Future Recommendations

This thesis presented the first step in developing a PM with which to explore the design space of an NPMS. The findings presented regarding the development and analysis of this model thus serve as the basis for four future research endeavors. The first is to model the NPMS hydrodynamics in greater detail by incorporating resistance and powering calculations, maneuvering transits, control

surfaces, and surface characteristics into the PM. The second is to improve the interface between the MathCAD model and the3D model and, as the model design progresses, using the MathCAD model to calculate NPMS characteristics in real time. The third is modeling the electrical power system and, based on the recognition that cost is nearly always an important, if not the most important, consideration, the fourth is developing a means by which to compare the costs that would be incurred in the realization of the different designs proposed for an NPMS.

Nomenclature

Below is a list of all terms and variables used in this thesis.

a	aft ballast tank major radius
A_{Hull}	hull wetted surface area
ABT	aft ballast tank
b	aft ballast tank minor radius
B_{aft}	batteries in the aft compartment
B_{fwd}	batteries in the forward compartment
B_H	battery height
B_L	battery length
BS_H	height of the bottomskin
B_W	battery width
BW	bulkhead bottom width
CB_x	center of buoyancy of the buoyancy pods
CCD	center composite design
CG	center of gravity
CG_{bow}	center of gravity of the bow dome
$CG_{tailcone}$	center of gravity of the tailcone
COTS	commercial-off-the-shelf
D_{max}	maximum depth
DDS	dry dock shelter
$Divers_{aft}$	number of divers in aft compartment
$Divers_{fwd}$	number of divers in forward compartment
DOE	design of experiments
DVL	Doppler velocity log
E_{5086}	elastic modulus, Al5086
E_{CF}	yield strength, carbon fiber
F_I	inner fillet radius of forward ballast tank
F_O	outer fillet radius of forward ballast tank
FBT	forward ballast tank

FEA	finite element analysis
g	acceleration of gravity
GDO	goal-driven optimization
h_{BH}	bulkhead height
h_{diver}	minimum diver height
h_{margin}	height margin
h_{max}	maximum allowable height
h_{NPMS}	NPMS height
h_{SB}	strongback height
h_w	longitudinal weldment height
HP	high pressure
L_{ABT}	aft ballast tank cylinder length
L_{AF}	air flask length
L_{DSL}	diver stack length
L_f	length of the bow section
L_{FBT}	length of forward ballast tank
L_{max}	maximum allowable length
L_{MDSL}	minimum diver stack length
L_{PMB}	length on the parallel middle body
LBP	lifting bearing plate
LM	load multiplier
M_i	point mass
MCP	minimum collapse pressure
NPMS	non-pressurized manned submersible
OAS	obstacle avoidance subsystem
OBT	open ballast tank
P	pressure
P_{AF}	air flask pressure
P_{crit}	critical pressure
PM	parametric model
r_{AF}	air flask radius
R	radius of forward ballast tank
R_x	longitudinal reaction force

R_Z	vertical reaction force
S	forward ballast tank stiffener height
SB_H	strongback height
SDV	SEAL delivery vehicle
SF	safety factor
SOF	special operating forces
SW	bulkhead side width
sw	specific weight of water, nominal
sw_{max}	specific weight of water, max
sw_{min}	specific weight of water, min
t_{ABT}	aft ballast tank thickness
t_{AF}	air flask wall thickness
t_{FBT}	wall thickness of forward ballast tank
t_{LBP}	thickness of the lifting bearing plate
TW	bulkhead top width
UBA	underwater breathing apparatus
V_{ABT}	volume of aft ballast tank
V_{AF}	air flask volume
V_{bow}	bow volume
V_{cargo}	cargo volume
V_{comp}	weight of a component
V_{diver}	diver volume
V_{FBT}	volume of forward ballast tank
V_{Hull}	hull volume
$V_{Tailcone}$	tailcone volume
V_{VBT}	volume of variable ballast tanks
VBT	variable ballast tank
VBT_{margin}	variable ballast tank margin
w_{BH}	bulkhead width
w_{margin}	width margin
w_{max}	maximum allowable width
w_{diver}	minimum diver width
W	weight

W_{air}	weight of air in airflasks
W_{batt}	*weight of a battery box*
W_{BS}	weight of bottom skin
W_{cargo}	cargo wet weight
W_{comp}	weight of a component
W_{NPMS}	weight on non-pressurized manned submersible
W_w	weight of water contained in the hull
WPI	weight per inch
$x_{aftbatt}$	longitudinal position of the aft battery point mass
$x_{fwdbatt}$	longitudinal position of the forward battery point mass
X_2	distance from bulkhead #1 to bulkhead #2
X_3	distance from bulkhead #1 to bulkhead #3
X_a	distance from aft end of the strongback to the center of the aft lifting point
X_f	distance from forward end of the strongback to the center of the forward lifting point
YS_{H116}	yield strength, al5086-h116
YS_O	yield strength, al5086-o
Z_{offset}	hull vertical offset
ηa	parabola exponent coefficient
ηf	ellipse exponent coefficient
ν	Poisson ratio
ρ_{5086}	density, Al5086
ρ_{CF}	density, carbon fiber
ρ_{foam}	buoyancy foam density
σ_1	tangential stress
σ_2	axial stress
σ_{Hull}	hull bending stress
σ_θ	Aft ballast tank membrane stresses in the direction of the meridian direction
σ_φ	Aft ballast tank membrane stresses in the direction of the equatorial direction
$\emptyset_{LP}$	diameter of lifting hole

References

[1] J. Greene, *The Black Prince and the Sea Devils.* Cambridge: Da Capo Press, 2004. pp. 4-7.

[2] Submarine Force Museum, (2011) *The Submarine Force Museum Virtual Tour* [Online]. Available: http://www.ussnautilus.org

[3] Naval Special Warfare Command.(2011). History [Online]. Available: http://www.navsoc.navy.mil/History.html.

[4] M. Slattery, "Spence Dry: A SEAL's Story," *The Naval Institute,* vol. 131, pp. 54-60, July 2005.

[5] N. Polmar, "The Naval Institute guide to the ships and aircraft of the U.S. fleet," ed. Annapolis, Md.: Naval Institute Press, 2005, p. 99.

[6] E. Wertheim, "The Naval Institute guide to combat fleets of the world: their ships, aircraft and systems," 15th ed. Annapolis, Md.: Naval Institute Press, 2007, pp. 99-100.

[7] P. Holzer, "Analysis and Design of a Non-Pressurized Manned Submersible," M.S. thesis, Mechanical Engineering Department, Massachusetts Institute of Technology, Cambridge, MA, 2011.

[8] American Special Operations. (2011). *SEAL Delivery Vehicle Teams* [Online]. Available: http://seals.americanspecialops.com/seal-delivery-vehicle-teams

[9] U.S. Special Operations Command, Shallow Water Combat Submersible (SWCS) Solicitation Number: H92222-10-R-0005F [Online]. Available: http://www.FedBizOpps.gov

[10] R. Burcher and L. Rydill, *Concepts in submarine design.* Cambridge England ; New York: Cambridge University Press, 1994.

[11] DIAB Group. (2011). *Divinycell H - The High Performance Core* [Online]. Available: http://www.diabgroup.com

[12] Teledyne Technologies. (2011). *Teledyne RD Instruments* [Online]. Available: http://www.rdinstruments.com

[13] O. F. Hughes , *Ship Structural Design : A rationally-based, computer-aided optimization approach*, [SNAME edition.] ed. Jersey City, N.J.: Society of Naval Architects and Marine Engineers, 1988. pp 1-128.

[14] ANSYS (2011),*"Introduction to ANSYS DesignXplorer 12.0"* [Online]. Available: https://www1.ansys.com

[15] J. G. Kaufman, *Introduction to Aluminum Alloys and Tempers.* Materials Park, OH: ASM International, 2000. pp 43-65.

[16] American Petroleum Institute , "API Spec 2C Specification for Offshore Pedestal Mounted Cranes," 6th ed: Tulsa, OK.:American Petroleum Institute. 2004

[17] H. A. Jackson, "Submarine Parametrics," presented at the Proc. Royal Inst. of Naval Archit. Internat. Symp. on Naval Submarines, 1983.

[18] Naval Sea Systems Command (1998) "SS800-AG-MAN-010/P-9290 System Certification Procedures and Criteria Manual for Deep Submergence Systems," ed: Commander, Naval Sea Systems Command.

[19] A. Blake, *Practical stress analysis in engineering design*, 2nd ed. New York: M. Dekker, 1990.

[20] S. Timoshenko and S. Woinowsky-Krieger, *Theory of Plates and Shells*, 2d ed. New York,: McGraw-Hill, 1959. pp. 466-497.

Appendix A - MathCAD Model

Design Inputs

General Parameters

$W_{max} := 0 \cdot in$

$H_{max} := 0 \cdot in$

$L_{max} := 0 \cdot in$

$L_{PMB} := 0 \cdot in$

$V_s := 0 \cdot kts$

$Cargo_{WW} := 0 \cdot lbf$

$sw_{max} := 64.5 \frac{lbf}{ft^3}$

$sw := 64 \frac{lbf}{ft^3}$

$sw_{min} := 62.5 \frac{lbf}{ft^3}$

$Cargo_{Vol} := 0 \cdot ft^3$

$\rho := 1000 \frac{kg}{m^3}$

$kts := .5144 \frac{m}{s}$

Battery Dimensions

$Battery_{Height} := 0 in$

$Battery_{Length} := 0 \cdot in$

$Battery_{Width} := 0 \cdot in$

$\rho_{Battery} := 0 \frac{lb}{ft^3}$

Diver Parameters

$Diver_{minh} := 0 \cdot in$

$Diver_{MSL} := 0 \cdot in$

$Diver_{SL} := 0 in$

$Diver_{fwd} := 0$

$Diver_{aft} := 0$

$Diver_{minw} := 0 \cdot in$

$Diver_{vol} := 0 ft^3$

$D_{max} := 0 \cdot ft$

Airflask Inputs

$V_{AF} := 0 \cdot in^3$

$P_{AF} := 0 \cdot psi$

$YS_{CF} := 5650 \cdot 10^6 \cdot Pa$

$SF_{AF} := 3$

$\rho_{CF} := 1.75 \frac{gm}{cm^3}$

Material Parameters

$SF_{tank} := 2$

$SF_{Hull} := 1.5$

$DLF := 2$

$SCF := 2.5$

$\rho_{ABS} := .0376 \frac{lb}{in^3}$

$\rho_{GRP} := 1740 \frac{kg}{m^3}$

$YS_{5086O} := 17 \cdot ksi$

$YS_{H116} := 30 \cdot ksi$

$E_{5086} := 10300 ksi$

$\nu := .3$

$\rho_{5086} := .096 \frac{lb}{in^3}$

$\rho_{foam} := 6 \frac{lbf}{ft^3}$

Hull Design Inputs

$Weldment_H := 0 \cdot in$

$L_f := 0 \cdot in$

$BS_H := 0 \cdot in$

$Tailcone_{thickness} := 0 \cdot in$

$Margin_H := 0 \cdot in$

$BS_t := 0 \cdot in$

$BH_t := 0 \cdot in$

Bulkhead Spacing

$$x_2 := \begin{cases} Diver_{MSL} & \text{if } Diver_{fwd} \le 2 \\ \left(\frac{Diver_{fwd}}{2} \cdot Diver_{SL}\right) & \text{otherwise} \end{cases}$$

$x_2 = \blacksquare \cdot in$

$$x_3 := \begin{cases} L_{PMB} - Diver_{MSL} & \text{if } Diver_{aft} \le 2 \\ \left[L_{PMB} - \left(\frac{Diver_{aft}}{2}\right) \cdot Diver_{SL}\right] & \text{otherwise} \end{cases}$$

$x_3 = \blacksquare \cdot in$

Batteries

$$Batteries_{fwd} := trunc\left(\frac{x_2}{Battery_{Width}}\right) = \blacksquare$$

Verification: Verify the total number of batteries meets vehicles power requirement.

$$Batteries_{aft} := trunc\left(\frac{L_{PMB} - x_3}{Battery_{Width}}\right) = \blacksquare$$

$$Batteries_{Vol} := Battery_{Width} \cdot Battery_{Height} \cdot Battery_{Length} \cdot \left(Batteries_{fwd} + Batteries_{aft}\right) = \blacksquare \cdot ft^3$$

AirFlasks

Weight of Air in Air Flasks when Fully Pressurized

$$Air_{Weight} := V_{AF}\frac{P_{AF}}{14.7\cdot psi}\frac{29\cdot gm\cdot g}{22.4\cdot L} =$$

$t := .5\cdot in$

$r := 5\cdot in$

User Input: Enter initial values for air flask radius and thickness.

$$l := L_{PMB} - x_2 + r = \blacksquare$$

$$Mass_{AF}(r,h,l) := \left[\frac{4}{3}\pi(r+t)^3 + \pi\cdot(r+t)^2(l-2\cdot r) - \frac{V_{AF}}{2}\right]\cdot\rho_{CF}$$

Giver

User Input: Enter constraints for the Airflask radius and thickness

$3\cdot in < r < 6\cdot in$

$.5\cdot in < t < 1\cdot in$

$L_{PMB} - x_2 + r + 5\cdot in > l > L_{PMB} - x_2 + r$

$$\frac{YS_{CF}}{SF_{AF}} > P_{AF}\frac{r}{t}$$

$$\frac{4}{3}\pi(r)^3 + \pi\cdot(r)^2(l-2\cdot r) = \frac{V_{AF}}{2}$$

$$\begin{pmatrix} AF_{radius} \\ AF_h \\ AF_{length} \end{pmatrix} := Minimize(Mass_{AF}, r, t, l) = \blacksquare\cdot in$$

Air Flask Parameters

$AF_{radius} = \blacksquare\cdot in$

$AF_h = \blacksquare\cdot in$

$AF_{length} = \blacksquare\cdot in$

$Mass_{AF}(AF_{radius}, AF_h, AF_{length}) = \blacksquare$

$$AF_{Vol} := \frac{4}{3}\pi(AF_{radius} + AF_h)^3 + \pi\cdot(AF_{radius} + AF_h)^2(AF_{length}) = \blacksquare\cdot ft^3$$

Hull Parameters

Vehicle Height

Verification: Verify H less than maximum H_{max}

$H := Weldment_H + Battery_{Height} + Diver_{minh} + 2 \cdot AF_{radius} + Margin_H = \blacksquare \cdot in$

$H_{max} = \blacksquare \cdot in$

Vehicle Width

Verification: Verify Width less than maximum W_{max}

$Width := 2 \cdot Diver_{minw} = \cdot in$

$W_{max} = \blacksquare \cdot in$

Length of Tailcone:

$L_a := L_{max} - (L_f + L_{PMB}) = \cdot in$

Bulkhead Parameters

$BH_{R3} := (Width - Battery_{Length}) = \blacksquare \cdot in$

$BH_{R1} := \frac{(Width - 2 \cdot AF_{radius})}{2} = \blacksquare \cdot in$

$BH_{RI4} := \frac{3}{4} BH_{R3} = \blacksquare \cdot in$

$BH_{RI1} := \frac{Width}{9} = \blacksquare \cdot in$

$BH_h := H - AF_{radius} = \blacksquare \cdot in$

$BH_{SW} := BH_{RI1}$

$BH_{BW} := BH_{RI1}$

$BH_{TW} := AF_{radius} \cdot 2 = \blacksquare \cdot in$

$Area_{bho} := BH_h \cdot Width - \pi \frac{BH_{R1}^2}{2} - \frac{\pi BH_{R3}^2}{2}$

$Area_{bhi} := (Width - 2 \cdot BH_{SW}) \cdot (BH_h - BH_{BW} - BH_{TW}) - \frac{\pi}{2} BH_{RI1}^2 - \frac{\pi}{2} \cdot BH_{RI4}^2$

$BH_{area} := Area_{bho} - Area_{bhi} = \blacksquare \cdot in^2$

$BH_{mass} := Area_{bho} \cdot BS_t \cdot \rho_{5086} = \blacksquare$

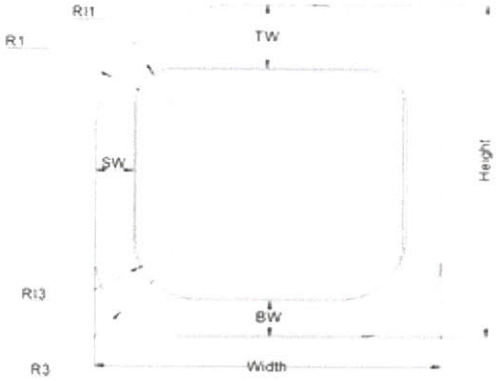

Bulkhead Parameters

$$BH_{Vol} := BH_{area} \cdot BS_t = \blacksquare \cdot ft^3$$

$$BH_{Perimeter} := \left(BH_h - BH_{R1} - BH_{R3}\right)2 + \left(Width - 2 \cdot BH_{R1}\right) + \left(Width - 2 \cdot BH_{R3}\right) + BH_{R1} \cdot \pi + BH_{R3} \cdot \pi = \blacksquare$$

$$BS_{mass} := BS_{area} \cdot in^2 \cdot L_{PMB} \cdot \rho_{5086} = \blacksquare \cdot lb$$

$$BS_{Vol} := BS_{area} \cdot in^2 \cdot L_{PMB} = \blacksquare \cdot ft^3$$

Hull Profile

$\eta f := 3$ User Input: Adjust to modify the fineness of bow

$\eta a := 1.7$ User Input: Adjust to modify fineness of tailcone

$$x1 := 0 \cdot in, .1 \cdot in .. \left(L_f + L_{PMB} + L_a\right)$$

$$zf(x1) := \left[1 - \left(\frac{L_f - x1}{L_f}\right)^{\eta f}\right]^{\frac{1}{\eta f}} \frac{BH_h}{2}$$

$$za(x1) := \left[1 - \left[\frac{x1 - \left(L_f + L_{PMB}\right)}{L_a}\right]^{\eta a}\right] \frac{BH_h}{2}$$

$$yb(x1) := \left[1 - \left[\frac{x1 - \left(L_f + L_{PMB}\right)}{L_a}\right]^{\eta a}\right] \frac{Width}{2}$$

$$off(x1) := if\left(x1 < L_f, zf(x1), \frac{BH_h}{2}\right)$$

$$off(x1) := if\left[x1 \le \left(L_f + L_{PMB}\right), off(x1), za(x1)\right]$$

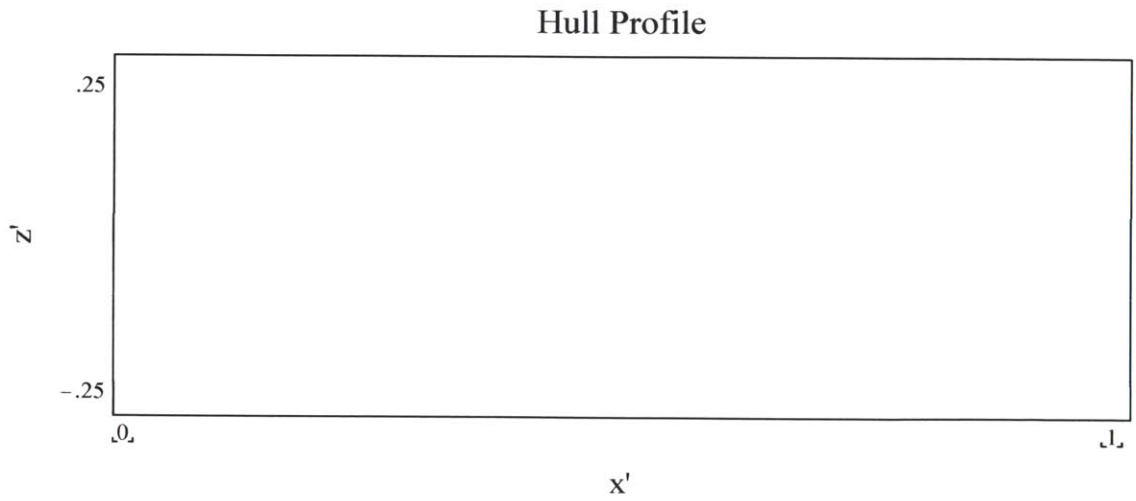

$$A_{ws} := \int_{0}^{L_f} off(x1) \cdot 2\pi \, dx1 + \int_{L_f+L_{PMB}}^{L_{max}} off(x1) \cdot 2\pi \, dx1 + BH_{Perimeter} \cdot L_{PMB} = \blacksquare \cdot ft^2$$

$$V_{tot} := \int_{0}^{L_f} off(x1)^2 \cdot \pi \, dx1 + \int_{L_f+L_{PMB}}^{L_{max}} off(x1)^2 \cdot \pi \, dx1 + Area_{bho} \cdot L_{PMB} = \blacksquare \cdot ft^3$$

$$Tailcone_{Vol} := \int_{L_f+L_{PMB}}^{L_{max}} off(x1)^2 \cdot \pi - \pi \left(off(x1) - Tailcone_{thickness}\right)^2 dx1 = \blacksquare \cdot in^3$$

$$Tailcone_{mass} := Tailcone_{Vol} \cdot \rho_{GRP} = \blacksquare$$

$$CG_{tailcone} := \frac{\int_{L_f+L_{PMB}}^{L_{max}} \left[off(x1)^2 \cdot \pi - \pi \left(off(x1) - Tailcone_{thickness}\right)^2\right] x1 \, dx1}{\int_{L_f+L_{PMB}}^{L_{max}} off(x1)^2 \cdot \pi - \pi \left(off(x1) - Tailcone_{thickness}\right)^2 dx1} = \blacksquare \cdot in$$

$$Bow_{Vol} := \int_{0}^{L_f} off(x1)^2 \cdot \pi - \pi \left(off(x1) - Tailcone_{thickness}\right)^2 dx1 = \blacksquare \cdot in^3$$

$$Bow_{mass} := Bow_{Vol} \cdot \rho_{ABS} = \blacksquare$$

$$CG_{bow} := \frac{\int_{0}^{L_f} \left[off(x1)^2 \cdot \pi - \pi \left(off(x1) - Tailcone_{thickness}\right)^2\right] x1 \, dx1}{Bow_{Vol}} = \blacksquare \cdot in$$

Loading Conditions and Strongback Calculations

$$Cargo_x := L_f + x_3 + \frac{L_{PMB} - x_3}{2} = \cdot in$$

$$CG_{BattFwd} := \frac{Batteries_{fwd} \cdot Battery_{Width}}{2} + L_f = \blacksquare \cdot in$$

$$CG_{BattAft} := \left(L_f + L_{PMB}\right) - \frac{Batteries_{aft} \cdot Battery_{Width}}{2} = \blacksquare \cdot in$$

$$W_{BattFwd} := Batteries_{fwd} \cdot Battery_{Width} \cdot Battery_{Length} \cdot Battery_{Height} \cdot \rho_{Battery} \cdot g = \blacksquare \cdot lbf$$

$$W_{BattAft} := Batteries_{aft} \cdot Battery_{Width} \cdot Battery_{Length} \cdot Battery_{Height} \cdot \rho_{Battery} \cdot g = \blacksquare \cdot lbf$$

$$Volume_{BS} := \left[\pi \frac{BH_{R3}^{\,2}}{2} + BH_{R3} \cdot \left(BS_H - BH_{R3}\right) + \left(Width - BH_{R3}\right) \cdot BS_H\right] L_{PMB} = \blacksquare \cdot in^3$$

$$Volume_{Batt} := \frac{W_{BattFwd} + W_{BattAft}}{\rho_{Battery} \cdot g}$$

$$Weight_{water} := sw \cdot \left(Volume_{BS} - Volume_{Batt}\right) = \blacksquare$$

$$Weight_{wpi} := \frac{Weight_{water} + BS_{mass} \cdot g}{L_{PMB}} = \blacksquare \frac{lbf}{in}$$

$$Weights := \begin{pmatrix} Weight_{water} \\ BS_{mass} \cdot g \\ BH1_{0,0} \cdot lbf \\ BH2_{0,0} \cdot lbf \\ BH3_{0,0} \cdot lbf \\ W_{BattFwd} \\ W_{BattAft} \end{pmatrix}$$

Vertical Lifting Force at each lifting point

$$R := \frac{\sum Weights}{2} = \blacksquare$$

Sum of the Moments about x=0

$$M_0(X_f, X_{ao}) := \begin{bmatrix} \frac{Weight_{water}}{lbf} & \frac{L_f + \frac{L_{PMB}}{2}}{in} \\ \frac{BS_{mass} \cdot g}{lbf} & \frac{L_f + \frac{L_{PMB}}{2}}{in} \\ BH1_{0,0} & BH1_{0,1} \\ BH2_{0,0} & BH2_{0,1} \\ BH3_{0,0} & BH3_{0,1} \\ \frac{W_{BattFwd}}{lbf} & \frac{CG_{BattFwd}}{in} \\ \frac{W_{BattAft}}{lbf} & \frac{CG_{BattAft}}{in} \\ \frac{-R}{lbf} & \frac{(X_f + L_f)}{in} \\ \frac{-R}{lbf} & \frac{(X_{ao} + L_f)}{in} \end{bmatrix}$$

Strongback Shear Function

$$Q(X_d, X_f, X_{ao}) := \begin{cases} 0 \text{ if } X_d < L_f \\ BH1_{0,0} \cdot lbf + Weight_{wpi} \cdot (X_d - L_f) \text{ if } L_f < X_d < L_f + X_f \\ \left[BH1_{0,0} \cdot lbf + Weight_{wpi} \cdot (X_d - L_f) - R\right] \text{ if } X_f + L_f \le X_d < CG_{BattFwd} \\ \left[BH1_{0,0} \cdot lbf + Weight_{wpi} \cdot (X_d - L_f) - R + W_{BattFwd}\right] \text{ if } CG_{BattFwd} \le X_d < BH2_{0,1} \cdot in \\ \left[BH1_{0,0} \cdot lbf + Weight_{wpi} \cdot (X_d - L_f) - R + W_{BattFwd} + BH2_{0,0} \cdot lbf\right] \text{ if } BH2_{0,1} \cdot in \le X_d < CG_{BattAft} \\ \left[\left[BH1_{0,0} \cdot lbf + Weight_{wpi} \cdot (X_d - L_f) - R + W_{BattFwd} + BH2_{0,0} \cdot lbf + W_{BattAft}\right]\right] \text{ if } CG_{BattAft} \le X_d < X_{ao} + L_f \\ \left[\left[BH1_{0,0} \cdot lbf + Weight_{wpi} \cdot (X_d - L_f) - R + W_{BattFwd} + BH2_{0,0} \cdot lbf + W_{BattAft} - R\right]\right] \text{ if } X_{ao} + L_f \le X_d < L_f + L_{PMB} \\ \left[BH1_{0,0} \cdot lbf + Weight_{wpi} \cdot (X_d - L_f) - R + W_{BattFwd} + BH2_{0,0} \cdot lbf + W_{BattAft} - R + BH3_{0,0} \cdot lbf\right] \text{ if } X_d = L_f + L_{PMB} \\ 0 \text{ if } X_d > L_f + L_{PMB} \end{cases}$$

Moment Function

$$MM(X_d, X_f, X_{ao}) := \int_0^{X_d} Q(X, X_f, X_{ao})\, dX$$

Strongback Lifting Point Calculations

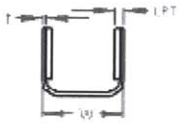

End Profile

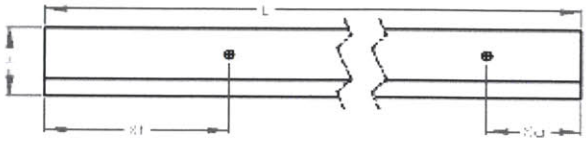

Side Profile

$X_f := 0 \cdot in$ $X_{ao} := 0 \cdot in$

$Offset := 5 \cdot in$ $X_d := 0 \cdot in$

User Input: Enter initial guess parameters. Adjust if solution does not converge. X_d is the initial guess for the expected location of the maximum moment. Offset is the minimum distance from the ends of the strongback.

Given

$80 \cdot in < X_d < L_f + L_{PMB}$

$Offset < X_f < 24 \cdot in$

$L_f + L_{PMB} - Offset > X_{ao} + L_f > CG_{BattAft} - .1 \cdot in$

$M_0(X_f, X_{ao})^{\langle 0 \rangle} \cdot M_0(X_f, X_{ao})^{\langle 1 \rangle} = 0$

$Results := Minimize(MM, X_d, X_f, X_{ao})$

Note: If solution fails to converge, adjust offset

$X_{ao} := Results_2 = 0 \cdot in$

Lifting Hole Locations

$X_f := Results_1 = 0 \cdot in$

$X_a := L_{PMB} - (X_{ao}) = 0 \cdot in$

Maximum Moment on the Strongback

$SB_{MaxMoment} := MM(Results_0, X_f, X_{ao}) = 0 \cdot lbf \cdot in$

$Results_0 = 0 \cdot in$

$X_d := 0 \cdot in, 1 in .. L_f + L_{PMB}$

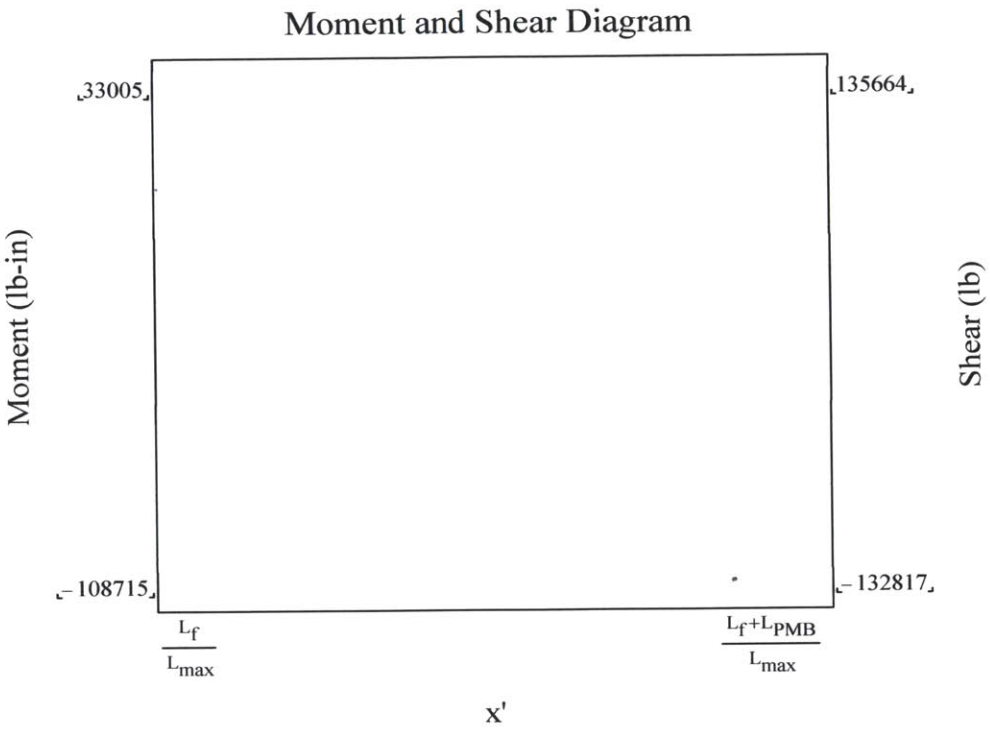
Moment and Shear Diagram
33005
135664
Moment (lb-in)
Shear (lb)
-108715
-132817
$\frac{L_f}{L_{max}}$
$\frac{L_f+L_{PMB}}{L_{max}}$
x'

Strongback Lifting Bearing Plate Calculations

Reference to Strongback Response Surface

Reference:C:\Users\Ken\Documents\MIT\Thesis\Hull Model\Strongback ResponseSurf

$SB_W := \blacksquare \cdot in$ $YS_{pin} := 30 \cdot ksi$ User Input: Enter SB_W and YS of lifting Pin

$SB_H := \blacksquare \cdot in$ $SB_t := \blacksquare \cdot in$ User Input: Initial guess values for strongback optimization

$LP_r := \blacksquare \cdot in$ $LP_t := \blacksquare \cdot in$

Response Function for the stress at the lifting point

$$\sigma_{SBLPT}(r,h,t) := C\left(\begin{pmatrix} r \\ t \\ h \end{pmatrix}\right) \frac{R \cdot DLF}{8500 in^2}$$

Giver

$\blacksquare \cdot in < LP_r < \blacksquare \cdot in$ User Input: Adjust Constraints as required to get solution to converge

$\blacksquare in < SB_H < \blacksquare in$

$SB_t < LP_t < \blacksquare \cdot in$

$$\frac{YS_{H116}}{SF_{Hull}} > \sigma_{SBLPT}\left(\frac{LP_r}{in}, \frac{SB_H}{in}, \frac{LP_t}{in}\right) > 0$$

$$\frac{YS_{pin}}{SF_{Hull}} > \frac{\frac{R}{2}}{\pi \cdot (LP_r)^2}$$

$Results_{SB} := Find(LP_r, SB_H, LP_t) = \blacksquare \cdot in$

Strongback Lifting Bearing Plate Dimensions:

$SB_H := Results_{SB_1} = \blacksquare \cdot in$

$LP_r := Results_{SB_0} = \blacksquare \cdot in$

$ALP_t := Results_{SB_2} = \blacksquare \cdot in$

Predicted Stress at the Lifting Points:

$$\sigma_{SBLPT}\left(\frac{LP_r}{in}, \frac{SB_H}{in}, \frac{ALP_t}{in}\right) = \blacksquare \cdot ksi$$

Strongback Properties

$$SB_{Area} := 2 \cdot SB_t \cdot SB_H + \left(SB_W - 2SB_t\right) SB_t$$

$$SB_{zbar} := \frac{SB_t \cdot SB_H^{\,2} + \left(SB_W - 2 \cdot SB_t\right) \frac{\left(SB_t\right)^2}{2}}{2 \cdot SB_t \cdot SB_H + \left(SB_W - 2SB_t\right) SB_t} = \blacksquare \cdot in$$

$$SB_{Iy} := \frac{2 \cdot SB_t \cdot SB_H^{\,3}}{12} + SB_t \cdot SB_H \cdot 2\left(\frac{SB_H}{2} - SB_{zbar}\right)^2 + \frac{\left(SB_W - 2 \cdot SB_t\right) \cdot SB_t^{\,3}}{12} + \left(SB_W - 2 \cdot SB_t\right) \cdot SB_t \cdot \left(SB_{zbar} - \frac{SB_t}{2}\right)^2 = \blacksquare \cdot in^4$$

$$SB_{mass} := SB_{Area} \cdot L_{PMB} \cdot \rho_{5086} = \blacksquare$$

$$SB_{Vol} := SB_{Area} \cdot L_{PMB} = \blacksquare \cdot ft^3$$

Hull Weldment Stress Calculations

Bending Stress on Hull Weldment

$$\sigma_{hullbottom}(x_d) := MM(x_d, X_f, X_{ao}) \frac{Z_{bar} \cdot in}{I_{Hull} \cdot in^4}$$

$$\sigma_{hullsb}(x_d) := MM(x_d, X_f, X_{ao}) \frac{-\left(BH_h + \frac{SB_H}{2} - Z_{bar} \cdot in\right)}{I_{Hull} \cdot in^4}$$

$$i := 0 .. trunc\left(\frac{L_f + L_{PMB}}{in}\right)$$

$$\sigma\sigma_i := \sigma_{hullsb}(i \cdot in)$$

Max/Min Bending Moments

max(σσ) =

min(σσ) =

Variable Ballast Tanks

$VB_{Margin} := .1$ User Input: VB Design Margin

$$VB := \left[Cargo_{WW} \frac{sw_{max}}{sw_{min}} + Air_{Weight} + \frac{W}{sw}\left(sw_{max} - sw_{min}\right) \right] \cdot \left(1 + VB_{Margin}\right) = \blacksquare \cdot lbf$$

$$D_{FBT} := \frac{x_3 - x_2}{2} + x_2 = \blacksquare \cdot in$$

$$D_{ABT} := L_{PMB} + 10 \cdot in$$

Initial Guess Values:

$$W_{ABT} := \frac{VB}{2} \qquad W_{FBT} := \frac{VB}{2}$$

Given $W_{ABT} \cdot \left(D_{ABT} - CG\right) = W_{FBT} \cdot \left(CG - D_{FBT}\right)$

$VB = W_{ABT} + W_{FBT}$

$W := Find\left(W_{FBT}, W_{ABT}\right) = \blacksquare \cdot lbf$

Required VBT volumes:

$$V_{FBT} := \frac{W_0}{sw} = \blacksquare \cdot ft^3$$

$$V_{ABT} := \frac{W_1}{sw} = \blacksquare \cdot ft^3$$

$FBT_{Length} := x_3 - x_2 = \cdot in$

$$P_{max} := D_{max} \cdot .444 \frac{psi}{ft} = 0 \cdot psi$$

$P_{Collapse} := P_{max} \cdot 1.5 = 0 \cdot psi$

Required OBT volume

$O\_VB := .25$ User Input: Enter OBT to VBT ratio

$OBT_{RB} := VB \cdot O\_VB = \blacksquare$

$$OBT_{Vol} := \frac{VB \cdot O\_VB}{sw} = \blacksquare \cdot ft^3$$

ABT Cylindrical

$$ml(a,h) := \frac{a}{h}$$

$$\zeta(x) := e^{-x}\cdot\sin(x)$$

$$\theta(x) := e^{-x}\cdot\cos(x)$$

$$\phi := \frac{E_{5086}}{YS_{5086O}}$$

$$Volume_{ABT}(a,b,L) := \frac{4}{3}\pi\cdot a^2\cdot b + \pi\cdot a^2(L)$$

$$Mass_{ABT}(a,b,h,L) := \rho_{5086}\left[\left(Volume_{ABT}(a,b,L)\right) - Volume_{ABT}(a-h,b-h,L)\right]$$

$$\sigma_{\varphi}(a,h) := P_{Collapse}\frac{a}{h}$$

$$\sigma_{\theta}(a,b,h) := \frac{P_{Collapse}\cdot a}{h}\left(1 - \frac{a^2}{2\cdot b^2}\right)$$

$$P_e(a,h,L) := YS_{5086O}\cdot e^{\left[\frac{-.815\left(\frac{a}{h}\right)^{.5}}{\frac{h}{L}\cdot\phi}\right]}\left[\left[\frac{1}{\left(\frac{a}{h}\right)^{.95}\cdot\left(\frac{h}{L}\cdot\phi\right)^{.1}}\right] - .01\cdot 2\frac{a}{h}\left[\frac{50}{\left(\frac{a}{h}\right)^{1.95}\cdot\left(\frac{h}{L}\cdot\phi\right)^{.1}} - \frac{33}{\left(\frac{a}{h}\right)^2}\right]\right]$$

$a := \blacksquare\cdot in$ $b := \blacksquare\cdot in$ $h := \blacksquare\cdot in$ $L := \blacksquare\cdot in$ User Input: Initial Values for optimization

Given

$a > b > 1\cdot in$

$\blacksquare\cdot in < h < \blacksquare\cdot in$

$\blacksquare\cdot in < a < \blacksquare\cdot in$

$Volume_{ABT}(a-h,b-h,L) = V_{ABT}$

$L + 2\cdot b < 2\cdot yb\left(L_{PMB} + L_f + 2a\right) - 2\cdot Tailcone_{thickness}$

$$\frac{-YS_{5086O}}{SF_{tank}} < \frac{P_{Collapse}\cdot a}{h}\left(1 - \frac{a^2}{2\cdot b^2}\right)$$

$P_{Collapse} < P_e(a,h,L)$

$$\begin{pmatrix} a \\ b \\ h \\ L \end{pmatrix} := \text{Minimize}(\text{Mass}_{ABT}, a, b, h, L) = \blacksquare \cdot \text{in}$$

ABT Parameters

$ABT_b := b = \blacksquare \cdot \text{in}$

$ABT_h := h = \blacksquare \cdot \text{in}$

$ABT_a := a = \blacksquare \cdot \text{in}$

$ABT_L := L = \blacksquare \cdot \text{in}$

ABT Properties

$ABT_{mass} := \text{Mass}_{ABT}(ABT_a, ABT_b, ABT_h, ABT_L) = \blacksquare$

$\sigma_\varphi(ABT_a, h) = \blacksquare \cdot \text{ksi}$

$\sigma_\theta(ABT_a, ABT_b, h) = \blacksquare \cdot \text{ksi}$

$P_e(ABT_a, ABT_h, ABT_L) = \blacksquare$

$\sigma_{VM}(\sigma_\varphi(ABT_a, h), \sigma_\theta(ABT_a, ABT_b, h)) = \blacksquare \cdot \text{psi}$

Stress Calculations in Cylindrical Section

$$\sigma_{xMax}(x) := \frac{a \cdot P_{Collapse}}{2 \cdot h} + \frac{3 \cdot a \cdot P_{Collapse} \frac{a^2}{2}}{4 \cdot h \sqrt{3(1 - \nu^2)}} \cdot \zeta(x)$$

$x := 2$ Note: Initial Gues

Giver

$x > 0$

$\beta x_{max} := \text{Maximize}(\sigma_{xMax}, x) = 0.785$

$\sigma_{xMax}(\beta x_{max}) = \blacksquare \cdot \text{ksi}$

$$\sigma_{tMax}(\beta x) := \frac{a \cdot P_{Collapse}}{h}\left[1 - \frac{1}{4}\frac{a^2}{b^2}\cdot\theta(\beta x) + 3\frac{\nu\frac{a^2}{b^2}}{4\sqrt{3\left(1-\nu^2\right)}}\cdot\zeta(\beta x)\right]$$

$\beta x := 1.8$

Given

$\beta x > 0$

$\beta x_{tmax} := \text{Maximize}(\sigma_{tMax}, \beta x) = 1.857$

$\sigma_{tMax}(\beta x_{tmax}) = \blacksquare \cdot ksi$

$\sigma_{VM}(\sigma_{tMax}(\beta x_{tmax}), \sigma_{xMax}(\beta x_{max})) = \blacksquare \cdot ksi$

Verification: Verify stress less than YS

$m := \frac{a}{h} = \blacksquare$ m>10 thin shell theory

$k := \frac{h}{ABT_L} = \blacksquare$

$\phi := \frac{E_{5086}}{YS_{5086O}} = 605.882$

$\lambda := 1.2\frac{\left(\frac{1}{4}\right)^m}{(k\cdot\phi)^{.5}}$ $\lambda = \blacksquare$

Forward Ballast Tank

$x_{BHFBT} := 0.0 \cdot in$ User Input: Adjust x_{BHFBT} for the allowable FBT distance into aft Compartment

$S := 3 \cdot in$ User Input: S is the stiffener height

Initial Values for optimization

$t := \blacksquare \cdot in$ User Input: Initial guess value for thickness

$Width_{FBT} := Diver_{minw}$

$H_1 := BH_h - Battery_{Height} - SB_H - Width_{FBT} = \blacksquare \cdot in$

$R_1 := \frac{Width_{FBT}}{2} = \cdot in$

$F_1 := \frac{3}{4} R_1 = \blacksquare \cdot in$

$L_1 := FBT_{Length} + x_{BHFBT} = \blacksquare \cdot in$

$$Volume_{FBT}(R_1, L_1, H_1, F_1) := \left(\pi \cdot R_1^2 + 2 \cdot H_1 \cdot R_1\right)(L_1 - 2 \cdot F_1) + \frac{\pi 4}{3}(F_1)^3 + \pi \cdot F_1^2(2R_1 - 2F_1) + 4 \cdot F_1 \cdot (2 \cdot R_1 + H_1 - 2 \cdot F_1)(R_1 - F_1) + \pi \cdot F_1^2 \cdot (2 \cdot R_1 + H_1 - 2 \cdot F_1)$$

$$Mass_{FBT}(R_1, L_1, H_1, F_1, t) := \left[Volume_{FBT}(R_1, L_1, H_1, F_1) - Volume_{FBT}(R_1 - t, L_1 - 2t, H_1, F_1 - t) + \left[2 \cdot \pi \left(R_1 - \frac{S}{2}\right) + 2H_1\right] \cdot S \cdot t\right] \cdot \rho_{5086}$$

Links to response surface data

Reference:C:\Users\Ken\Documents\MIT\Thesis\Hull Model\FBT ResponseSurf

Reference:C:\Users\Ken\Documents\MIT\Thesis\Hull Model\FBT Respon:

Giver

$$\blacksquare \cdot in \le t \le \blacksquare \cdot in$$

$$R_1 < \frac{Width_{FBT}}{2.0}$$

$$\frac{R_1}{2} < F_1 < R_1$$

$$L_1 < FBT_{Length} + x_{BHFBT}$$

$$V_{FBT} = Volume_{FBT}\left(R_1 - t, L_1 - 2t, H_1, F_1 - t\right) - \left[2 \cdot \pi \left(R_1 - \frac{S}{2}\right) + 2H_1\right] \cdot S \cdot$$

$$H_1 - 2 \cdot R_1 < BH_h - Battery_{Height} - SB_H - Weldment_H$$

$$H_1 < \frac{L_1}{2}$$

$$\sigma_{FBTS}\left(\frac{H_1}{in}, \frac{t}{in}, \frac{S}{in}, \frac{L_1}{in}\right) \frac{P_{Collapse}}{135} < \frac{YS_{H116}}{SF_{tank}}$$

$$\sigma_{FBTF}\left(\frac{R_1}{in}, \frac{t}{in}, \frac{F_1}{in}\right) \frac{P_{Collapse}}{135} < \frac{YS_{H116}}{SF_{tank}}$$

$$Results := Minimize\left(Mass_{FBT}, R_1, L_1, H_1, F_1, t\right)$$

FBT Parameters

$$FBT_{R1} := Results_0 = \blacksquare \cdot in$$

$$FBT_{H1} := Results_2 = \blacksquare \cdot in$$

$$FBT_t := Results_4 = \blacksquare \cdot in$$

$$FBT_{L1} := Results_1 = \blacksquare \cdot in$$

$$FBT_{F1} := Results_3 = \blacksquare \cdot in$$

FBT Properties

$$FBT_{mass} := Mass_{FBT}\left(FBT_{R1}, FBT_{L1}, FBT_{H1}, FBT_{F1}, FBT_t\right) = \blacksquare$$

$$V_{FBT} = \blacksquare \cdot in^3$$

$$\sigma_{FBTS}\left(\frac{FBT_{H1}}{in}, \frac{FBT_t}{in}, \frac{S}{in}, \frac{FBT_{L1}}{in}\right) \frac{P_{Collapse}}{135} = \blacksquare \cdot ksi$$

$$\sigma_{FBTF}\left(\frac{FBT_{R1}}{in}, \frac{FBT_t}{in}, \frac{FBT_{F1}}{in}\right) \frac{P_{Collapse}}{135} = \blacksquare \cdot ksi$$

Hull Layout

$FBTZ := \blacksquare \cdot in$

$AFZ := AF_{radius} + 1 \cdot in$

$ABTZ := \blacksquare \cdot in$

$ABTX := AF_{radius} \cdot 2 + 2 \cdot in$

$AFY := \frac{SB_W}{2} + AF_{radius} + 1in = \blacksquare \cdot in$

Design Convergence

CG Convergence

$$C := \begin{pmatrix} \frac{SB_{mass}}{lb} & \frac{L_f + \frac{L_{PMB}}{2}}{in} \\ \frac{BS_{mass}}{lb} & \frac{L_f + \frac{L_{PMB}}{2}}{in} \\ \frac{BH_{mass}}{lb} & \frac{L_f}{in} \\ \frac{BH_{mass}}{lb} & \frac{L_f + x_3}{in} \\ \frac{BH_{mass}}{lb} & \frac{L_f + L_{PMB}}{in} \\ BH1_{0,0} & BH1_{0,1} \\ BH2_{0,0} & BH2_{0,1} \\ BH3_{0,0} & BH3_{0,1} \\ \frac{W_{BattFwd}}{lbf} & \frac{CG_{BattFwd}}{in} \\ \frac{W_{BattAft}}{lbf} & \frac{CG_{BattAft}}{in} \\ \frac{FBT_{mass}}{lb} & \frac{D_{FBT}}{in} \\ \frac{ABT_{mass}}{lb} & \frac{D_{ABT}}{in} \\ 0 & 0 \end{pmatrix}$$

$$CG_{intial} := \frac{\frac{L_{max}}{1.85} + \frac{L_{PMB}}{2}}{2} = \cdot in$$

Vehicle Weight

$$\sum C^{\langle 0 \rangle} \cdot lbf = \blacksquare \cdot lbf$$

$$CG_{calc} := \frac{C^{\langle 0 \rangle} \cdot C^{\langle 1 \rangle}}{\sum C^{\langle 0 \rangle}} = \blacksquare$$

$CG \equiv \blacksquare \cdot in$ User Input: Adjust CG value until it converges with CGcalc

Volume and Buoyancy Convergence

$$V := \begin{pmatrix} AF_{Vol} \\ Batteries_{Vol} \\ \frac{VB}{sw} \\ BH1_{0,5} \cdot in^3 \\ BH2_{0,5} \cdot in^3 \\ BH3_{0,5} \cdot in^3 \\ 0 \\ 3BH_{Vol} \\ SB_{Vol} \\ BS_{Vol} \\ 0 \end{pmatrix}$$

$$W_{total} := \sum C^{\langle 0 \rangle} \cdot lbf + Cargo_{WW} = \blacksquare$$

$$Buoyancy := W_{total} - \sum V \cdot sw = \blacksquare$$

$$Buoyancy_{vol} := \frac{Buoyancy}{sw} = \blacksquare \cdot ft^3$$

$$Bouyancy_{weight}\left(Buoyancy_{vol}\right) := Buoyancy_{vol} \cdot \rho_{foam}$$

Given

$$\sum C^{\langle 0 \rangle} \cdot lbf + Cargo_{WW} + Bouyancy_{weight}\left(Buoyancy_{vol}\right) = sw \cdot Buoyancy_{vol} + \sum V \cdot sw$$

Required Buoyancy Foam

$$Buoyancy_{vol} := Find\left(Buoyancy_{vol}\right) = \blacksquare \cdot ft^3$$

$$V := \begin{bmatrix} AF_{Vol} \\ Batteries_{Vol} \\ Buoyancy_{vol} \\ BH1_{0,5} \cdot in^3 \\ BH2_{0,5} \cdot in^3 \\ BH3_{0,5} \cdot in^3 \\ Diver_{vol} \cdot (Diver_{aft} + Diver_{fwd}) \\ 3BH_{Vol} \\ SB_{Vol} \\ BS_{Vol} \\ Cargo_{Vol} \\ OBT_{Vol} \\ 0 \end{bmatrix}$$

$\sum V = \blacksquare \cdot ft^3$ $V_{tot} = \blacksquare \cdot ft^3$ Verification: Verify left side is smaller than right side

Appendix B MathCAD Strongback Response Surface Results

The response surface is a 3rd degree polynomial in the form:

$$\sigma(p1, p2..pn) = C_{intercept} + C_{p1} \cdot p1 + \cdots + C_{pn} \cdot pn + C_{p1p2} \cdot p1p2 \ldots$$

Using the *polyfit* command in MathCAD, the following coefficients and ANOVA results were generated.

Term	Coefficient	Std Error	95% CI Low	95% CI High	VIF	T	P
Intercept	-5.10E+06	1.35E+06	-8.56E+06	-1.64E+06	NaN	-3.785	6.57E-03
R	-1.34E+06	6.80E+05	-3.09E+06	4.10E+05	4.90E+03	-1.968	0.068
t	1.24E+07	3.55E+06	3.24E+06	2.15E+07	8.56E+04	3.484	9.43E-03
H	7.93E+05	3.79E+05	-1.80E+05	1.77E+06	9.99E+04	2.095	0.057
RR	2.97E+06	1.44E+06	-7.41E+05	6.67E+06	2.24E+04	2.057	0.06
tt	-1.55E+07	4.50E+06	-2.71E+07	-3.94E+06	3.54E+05	-3.447	9.87E-03
HH	-9.97E+04	4.80E+04	-2.23E+05	2.38E+04	4.13E+05	-2.075	0.059
RRR	-2.08E+06	9.60E+05	-4.55E+06	3.89E+05	6.57E+03	-2.165	0.052
ttt	6.40E+06	1.88E+06	1.57E+06	1.12E+07	9.22E+04	3.41	0.01
HHH	4.11E+03	2.00E+03	-1.03E+03	9.25E+03	1.08E+05	2.054	0.061

Where r is the radius of the lifting point hole, t is the thickness of the lifting bearing plate, and H is the height of the strongback.

Regression Analysis	Value
Standard Deviation	5.96E+03
R2	0.916
Adjusted R2	0.704

The following plots show the response to varying each of the strongback parameters (r, t, H) individually for the nominal reaction force, R_z.

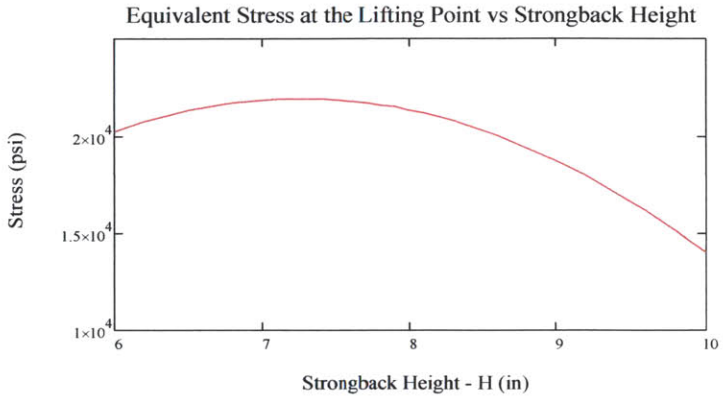
Equivalent Stress at the Lifting Point vs Strongback Height
Stress (psi)
2×10^4
1.5×10^4
1×10^4
6
7
8
9
10
Strongback Height - H (in)

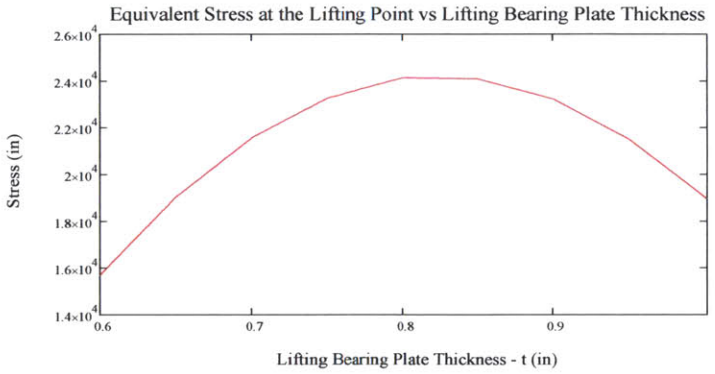
Equivalent Stress at the Lifting Point vs Lifting Bearing Plate Thickness
Stress (in)
2.6×10^4
2.4×10^4
2.2×10^4
2×10^4
1.8×10^4
1.6×10^4
1.4×10^4
0.6
0.7
0.8
0.9
Lifting Bearing Plate Thickness - t (in)

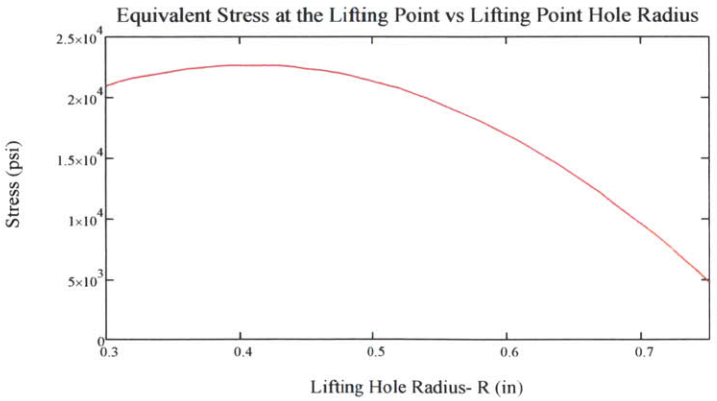
Equivalent Stress at the Lifting Point vs Lifting Point Hole Radius
Stress (psi)
2.5×10^4
2×10^4
1.5×10^4
1×10^4
5×10^3
0
0.3
0.4
0.5
0.6
0.7
Lifting Hole Radius- R (in)

Appendix C MathCAD Forward Ballast Tank Response Surface Results

Front Panel Response Surface

The response surface is a 2rd degree polynomial in the form:

$$\sigma(p1, p2..pn) = C_{intercept} + C_{p1} \cdot p1 + \cdots + C_{pn} \cdot pn + C_{p1p2} \cdot p1p2 \ldots$$

In this case, the stress on the FBT front panel is given by:

$$\sigma_{Front}(r, t, f) = C_{intercept} + C_r \cdot r + C_t \cdot t + C_f \cdot f + C_{rt} \cdot rt + C_{rf} \cdot rf + C_{tf} \cdot tf + C_{rr} \cdot r^2 + C_{tt} \cdot t^2 + C_{ff} \cdot f^2 \qquad (C.1)$$

Using the *polyfit* command in MathCAD, the following coefficients and ANOVA results were generated.

Term	Coefficient	Std Error	95% CI Low	95% CI High	VIF	T	P
$C_{Intercept}$	6.54E+03	1.10E+04	-1.57E+04	2.88E+04	NaN	0.597	0.33
C_r	8.36E+03	1.66E+03	4.98E+03	1.17E+04	312.166	5.03	2.35E-05
C_t	-5.09E+04	1.25E+04	-7.63E+04	-2.56E+04	198.119	-4.085	3.66E-04
C_f	-5.36E+03	1.48E+03	-8.35E+03	-2.36E+03	201.174	-3.633	1.27E-03
C_{rt}	-1.18E+04	797.245	-1.34E+04	-1.02E+04	102.828	-14.806	0
C_{rf}	-419.114	118.764	-660.472	-177.756	303.35	-3.529	1.68E-03
C_{tf}	1.20E+04	873.561	1.02E+04	1.38E+04	75.815	13.739	2.05E-15
C_{rr}	287.912	82.733	119.778	456.046	303.127	3.48	1.92E-03
C_{tt}	3.51E+04	9.10E+03	1.66E+04	5.36E+04	131.632	3.855	6.96E-04
C_{ff}	-45.608	106.97	-262.997	171.781	255.081	-0.426	0.361

Regression Analysis	Value
Standard Deviation	740.045
R2	0.992
Adjusted R2	0.99
Predicted R2	0.987

FBT Side Stress

The response surface is a 2rd degree polynomial in the form:

$$\sigma(p1, p2..pn) = C_{intercept} + C_{p1} \cdot p1 + \cdots + C_{pn} \cdot pn + C_{p1p2} \cdot p1p2 \ldots$$

In this case, the stress on the FBT side panel is given by:

$$\sigma_{Side}(h, t, s, l)$$

Using the *polyfit* command in MathCAD to generate the response surface for the function, the following coefficients and ANOVA results were generated:

Term	Coefficient	Std Error	95% CI Low	95% CI High	VIF	T	P
$C_{intercept}$	-5.21E+03	9.84E+03	-2.72E+04	1.67E+04	NaN	-0.53	0.334
C_h	825.81	442.624	-160.417	1.81E+03	323.112	1.866	0.075
C_t	1.07E+04	1.15E+04	-1.48E+04	3.63E+04	357.032	0.937	0.245
C_s	142.392	3.80E+03	-8.33E+03	8.62E+03	630.043	0.037	0.389
C_l	27.403	364.862	-785.56	840.367	493.997	0.075	0.388
C_{ht}	-992.962	240.779	-1.53E+03	-456.474	51.347	-4.124	1.65E-03
C_{hs}	-85.417	60.195	-219.539	48.705	90.787	-1.419	0.142
C_{hl}	23.255	6.521	8.725	37.785	71.133	3.566	4.27E-03
C_{ts}	789.996	1.48E+03	-2.51E+03	4.09E+03	95.687	0.533	0.334
C_{tl}	-804.621	160.519	-1.16E+03	-446.962	76.034	-5.013	3.88E-04
C_{sl}	-23.82	40.13	-113.235	65.594	115.474	-0.594	0.322
C_{hh}	-8.822	13.766	-39.494	21.85	181.015	-0.641	0.312
C_{tt}	4.63E+03	8.34E+03	-1.40E+04	2.32E+04	219.835	0.554	0.329
C_{ss}	32.912	521.307	-1.13E+03	1.19E+03	532.286	0.063	0.388
C_{ll}	15.088	6.118	1.456	28.72	376.586	2.466	0.029

Regression Analysis	Value
Standard Deviation	310.449
R2	0.995
Adjusted R2	0.989
Predicted R2	0.976

The following plots show the response while varying each parameter individual for a nominal external pressure.